DISSERTATION

TWO TYPES OF MELANOPSIN RETINAL GANGLION CELL IN THE MOUSE RETINA: THE REGULATION OF MELANOPSIN EXPRESSION

Submitted by

Scott Benjamin Baver

Department of Biomedical Sciences

In partial fulfillment of the requirements

For the Degree of Doctor of Philosophy

Colorado State University

Fort Collins, Colorado

Fall 2009

COLORADO STATE UNIVERSITY

November 10, 2009

WE HEREBY RECOMMEND THAT THE DISSERTATION PREPARED UNDER OUR SUPERVISION BY SCOTT BAVER ENTITLED "TWO TYPES OF MELANOPSIN RETINAL GANGLION CELL IN THE MOUSE RETINA: THE REGULATION OF MELANOPSIN EXPRESSION" BE ACCEPTED AS FULFILLING IN PART REQUIREMENTS FOR THE DEGREE OF DOCTOR OF PHILOSOPHY.

Committee on Graduate Work

Kathryn M. Partin

Deborah M. Garrity

Jozsef Vigh

Advisor: Stuart Tobet

Department Head: Barbara M. Sanborn

ABSTRACT OF DISSERTATION

TWO TYPES OF MELANOPSIN RETINAL GANGLION CELL IN THE MOUSE RETINA: THE REGULATION OF MELANOPSIN EXPRESSION

Rods, cones and a subset of retinal ganglion cells (RGCs) that express the photopigment melanopsin are the sensory photoreceptors of the mammalian retina. The light-driven signals that are initiated by the photoreceptors are relayed from the retina to the brain. In addition to the role of light information in regulating the perception of colors, objects and movement, it also controls pupil size and the synchronization of daily physiological rhythms to the day/night cycle. The melanopsin-expressing RGCs, which are intrinsically photosensitive (ipRGCs), contribute especially to these two latter processes. The focus of this dissertation is the ipRGCs of the mouse retina.

While previous evidence has suggested that there are several ipRGC types in the mouse retina, there has been little supporting data to separate these cells into distinct types. Conventional RGC classification is based on a variety of parameters that includes soma size, dendrite branching, and dendrite ramification in the inner plexiform layer (IPL). It has proven difficult to use the same classification scheme for ipRGCs due to their extensive dendritic fields.

Chapter 2 identifies two types of ipRGC in the mouse retina using a mouse in which the *tau-lacZ* fusion protein replaces the melanopsin protein. These ipRGC types (M1 and M2) differentially project to the suprachiasmatic nucleus (SCN) of the hypothalamus and olivary pretectal nucleus (OPN). In addition, M1-type ipRGC dendrites ramify in the OFF sublamina while M2-type ipRGC dendrites ramify in the ON sublamina of the IPL. To further assess the role of classical photoreceptor pathways in regulating melanopsin expression, transgenic and reporter mouse lines were used and subjected to various lighting paradigms.

Chapter 3 explores the role of rod and cone photoreceptor pathway development on melanopsin levels in ipRGCs. In the mouse, rod and cone photoreceptor pathways are not fully developed until roughly postnatal day (PD) 10. Different ipRGC types are not evident at birth, and evidence obtained from two independent reporter mouse lines indicated that the separation of ipRGCs into two distinct types did not occur until PD 10. The development of M1 and M2 ipRGCs also is shown to depend on the daily light/dark cycle and dopaminergic neurotransmission.

In conclusion, the data presented in this dissertation indicate that there are two anatomically distinct ipRGC types in the mouse retina expressing differential amounts of melanopsin protein. Furthermore, the photoreceptors in the outer retina have a major role in regulating the amount of melanopsin protein that is present in ipRGCs. This regulation may be important for shaping the irradiance

information that is relayed to the brain and used to synchronize circadian rhythms to the light/ dark cycle and control pupil size.

Scott Baver
Department of Biomedical Sciences
Colorado State University
Fort Collins, CO 80523
Fall 2009

Acknowledgements

I would like to thank the neuroscience community at Colorado State University for their guidance, direction and commitment to my success as a researcher throughout my time as a graduate student. In particular I would like to thank Drs. Vigh, Tamkun, Tobet, Hentges and Partin for their absolutely amazing guidance throughout my graduate school experience. I would also like to thank everyone in the laboratory including Dr. Andrew Hartwick for helping me design the experiments presented in Chapters 3 and 4, as well as long thoughtful conversations throughout his tenure at Colorado State University. I also thank Dr. Malcolm Ogilvie, Dr. Jayne Bramley, Connie King, Allison Evans and Anne Simpson. Each of you has helped me complete my research and taught me how to work in a research environment, which will prove priceless as I move to the next step of my life. I am gratefully indebted to Dr. Ignacio Provencio who inspired me to find a technique to reliably differentiate ipRGCs.

I would like to thank my committee members Kathy Partin, Deborah Garrity and Jozsef Vigh for their support and advice on not only my project, but also my career here and my future endeavors. This also needs to be extended to Dr. Katherine V. Fite and Dr. Jozsef Vigh who not only took valuble time to discuss my ideas and edit Chapters of my thesis but also guided me through to the next step of my career. Dr. Andrew Hartwick is again acknowledged for reading and evaluating the entire thesis. This was also extended to my fellow graduate students who have helped me in my ability to critically grow scientifically and as a man. Several confocal images were collected with the assistance/expertise of

Shannon Gallagher. Without Shannon's kindness and patience I wouldn't have any figures in Chapter 3. Finally, I would like the acknowledge all of my friends and family that helped me through the past three years of graduate school. In particular I would like to thank Amy Blass for dealing with 'all of this' and can not begin to express my love and appreciation for all the 'craziness' I have put her through my past few years as a Ph.D student, thank you.

It has been quite a trip and all of you have helped me strive through the great times and the low times of my time here. I would never have made it through this portion of my life without you.

Sincerely,

Scott B. Baver

TABLE OF CONTENTS

List of Tables

Table of Figures

Chapter 1

Introduction

Light has a profound effect on many vertebrate physiological processes.

Visual perception is the major sensory role of the vertebrate eye, which allows an organism to obtain information about its surroundings by sensing light being reflected off objects. Perception of objects, hues, depth and motion begins with photon capture at the level of the neural retina. The signal is relayed to the lateral geniculate nucleus and further on to the visual cortex. In many vertebrates and especially primates a vast majority of the cortex is devoted to visual perception.

Other visual behaviors not classified as image forming perceptions include synchronization of activity rhythms to the light/ dark cycle and pupil constriction. This so called 'non-image forming' visual subsystem relies, in part, on illumination cues sent to non-image forming brain centers by a recently discovered photoreceptor in the mammalian retina. The intricate neural circuitries regulating non-image forming visual behaviors have become the center of research for many circadian biologists as well as visual neuroscientists.

There are three photoreceptor types in the mammalian retina.

The visual system can be divided into two visual subsystems: 1) the 'image-forming' and 2) the 'non-image-forming'. The latter subsystem relies on photon capture as the sensory stimulus that begins at the level of the neural retina. The image-forming subsystem, with regard to retinal anatomy, has been

well characterized (Boycott and Wässle, 1999; Masland, 2001; Wässle, 2004; Field and Chichilnisky, 2007). In mammals, visual perception begins with activation of rod photoreceptors in dim light and cone photoreceptors in daylight. The flow of information is transmitted to retinal ganglion cells (RGCs) via retinal interneurons (i.e. horizontal, bipolar and amacrine cells) (Masland, 2001). RGC axons project to visual centers in the brain (i.e. lateral geniculate nucleus) for higher-order visual processing.

Non-image forming behaviors include entrainment of circadian rhythms, pupillary light reflex (Lucas et al., 2001), masking responses (Mrosovsky and Hattar, 2003) and regulation of pineal melatonin synthesis (Lucas et al., 1999; Foster and Hankins, 2002). While rod and/or cone photoreceptor activation is sufficient for signaling to non-image forming visual centers it is not essential (von Schantz et al., 2000; van Gelder, 2003). A recently characterized RGC type, which is intrinsically photosensitive and contains the photopigment melanopsin, also relays illumination information to non-image forming visual nuclei (Berson, 2003). Although under active investigation, the retinal anatomical organization associated with the non-image forming subsystem remains incompletely understood.

The flow of information in the retina is vertical and lateral

There are two main pathways of chemical transmission in the mammalian retina that lead to signaling to the brain (Figure 1.1). In darkness, rod and cone photoreceptors are slightly depolarized (~-40 mV) resulting in constant release of the neurotransmitter glutamate (Trifinov, 1968; Kaneko and Shimazaki, 1976). The light sensitive pigments located on photoreceptor outer segments are comprised of an opsin and the chromophore retinal. On photon absorption, photoreceptors hyperpolarize resulting in cessation of glutamate release. In the case of cone photoreceptors, the signal is transmitted to second order retinal neurons known as the bipolar cell class. Bipolar cells located in the inner nuclear layer (INL) collect photopic information from cone photoreceptors and relay this information to RGCs. This 'direct pathway' (cone photoreceptor → bipolar cell → RGC) is one of the vertical retinal pathways. The vertical pathway is modified by lateral inhibition by two types of inhibitory retinal neurons. These neurons are termed the horizontal and amacrine cells and they release inhibitory neurotransmitters, glycine and γ- aminobutyric acid (GABA) accounting for the indirect 'lateral' pathway of retinal information processing. In mammals, there are ~ 25 different amacrine cell types (Mariani, 1990; Kolb et al. 1992). Several other neuroactive substances are co-released in amacrine cells including substance P, β-endorphin and dopamine.

Rod photoreceptors utilize a different pathway to convey stimuli very low in ambient light to the brain for processing. On light stimulation, rod photoreceptors signal ON-type rod bipolar cells and this information is primarily sent to two amacrine cell types, called AII and A17 amacrine cells. The AII amacrine cell communicates with cone bipolar cells to relay scotopic light information to RGCs while A17 amacrine cells are making direct inhibitory contact back to the rod bipolar cells, forming a "reciprocal" inhibitory feedback synapse (Bloomfield and Dachaeux, 2001, Chavez et al, 2006).

The ON-OFF parallel pathways of the mammalian retina segregate light increments and decrements.

As diagramed in Figure 1.1, the signaling of cones in the outer retina occurs at the first synaptic layer termed the outer plexiform layer (OPL). Communication between bipolar, amacrine and RGCs is accomplished in the second neuropil layer in the inner retina, known as the inner plexiform layer (IPL). Two distinct functional channels originally suggested by Barlow (1953) and Kuffler (1953) result in cells contributing to the ON and OFF pathways. These pathways signal varying levels of ambient light and are the first steps in visual perception.

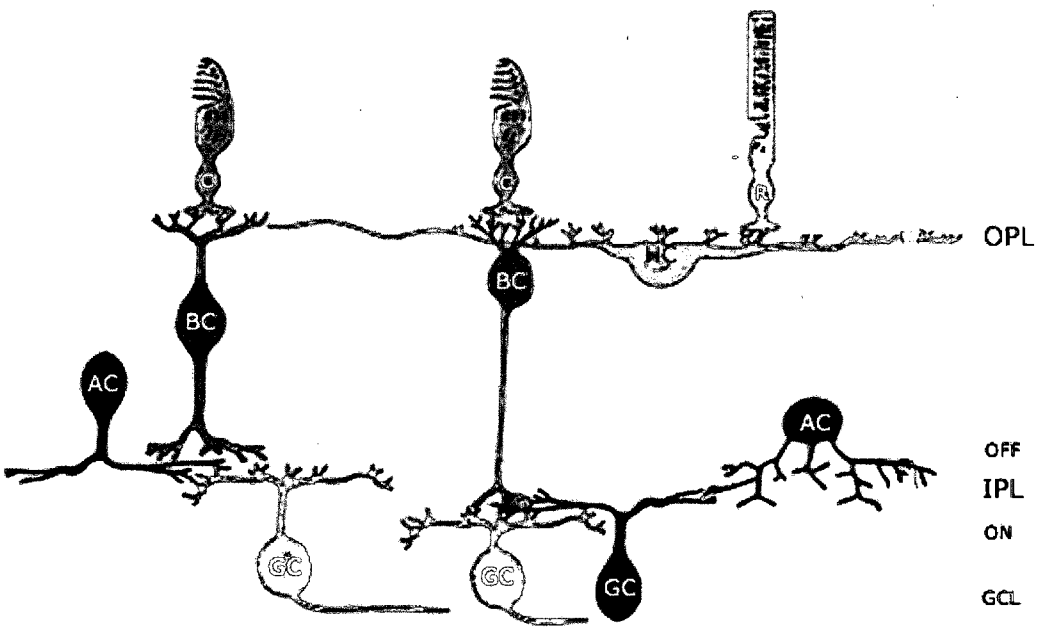

Figure 1.1. A schematic representation of the mammalian retina. Light enters the retina through the retinal ganglion cells in the ganglion cell layer (GCL) and continues until it reaches photosensitive retinal neurons called rods (R) and cones (C). On light stimulation, cone photoreceptors signal bipolar cells (BC) and horizontal cells (HC) in the first synaptic layer called the outer plexiform layer (OPL). BC information is sent to RGCs in vertical retinal pathway transmission. Amacrine cells (AC) receive signals from BC and communicate with RGCs and other AC and bipolar cells in the lateral pathway. Bipolar cells and AC axons contact RGCs dendrites in the inner plexiform layer (IPL). The IPL is segregated into two distinct sublamina (a and b) based on BC response to light. BCs that depolarize to light onset send axons that stratify in the ON sublamina of the IPL while BCs that depolarize to light offset send axons that stratify in the OFF sublamina of the IPL. RGCs gather all photic information from the outer retina and send it to visual brain centers for higher order processing.

The ON and OFF visual pathways begin at the photoreceptor- bipolar synapse

A fundamental feature of the vertebrate retina is that some cells respond to light increments (ON-responding cells) while other cells respond to light decrements (OFF-responding cells). These spiking patterns were first observed in RGC axons of the frog by Hartline (1938), although the origin of ON and OFF pathway segregation in the retina was not known until the work of Werblin and Dowling (1969). Using a fine electrode tip to record from various retinal cell types after light stimulation, Werblin and Dowling (1969) demonstrated that photoreceptors respond only in a graded fashion to light flux. Two major bipolar cell classes could be identified: cells that depolarize in response to light onset and cells that hyperpolarize in response to light onset.

As noted previously, photoreceptors release the neurotransmitter glutamate in the dark (Trifinov, 1968; Kaneko and Shimazaki, 1976). The presence (dark) or absence (light) of glutamate is encoded by second order retinal neurons, the bipolar cell (Werblin and Dowling, 1969). OFF bipolar cells are depolarized in complete darkness due to the presence of ionotropic glutamate receptors (iGluR), including α-amino-3-hydroxyl-5-methyl-4-isoxazole-propionate (AMPA) and kainate receptors. Upon light stimulation, OFF bipolar cells become hyperpolarized (Saito and Kaneko, 1983). Conversely, ON bipolar cells express metabotropic glutamate receptors (mGluR6) (Nawy and Jahr, 1990; Shiells and Falk, 1990). Several transduction pathway(s) suggested leading to depolarization of ON-bipolar cells in response to the light-triggered reduction of synaptic glutamate in the OPL (e.g. cGMP regulating calcium channels) (Nawy and Jahr,

1990; Shiells and Falk, 1990). To date, the molecular pathway from mGluR6 activation to bipolar cell neurotransmitter realease is not completely understood (Snellman et al., 2008). Importantly, the ON and OFF responses observed in bipolar cells are mirrored by RGC types respnding to light increments and light decrements (Hartline, 1938).

There is an anatomical substrate for ON and OFF responding neurons

The IPL is a milieu of bipolar and amacrine cell axons that synapse upon RGC dendrites. Anatomical studies have demonstrated distinct structural characteristics between ON and OFF bipolar cells (Rodieck, 1973; Famiglietti et al., 1977; Wässle and Boycott, 1981a,b). ON and OFF bipolar cell axons stratify in distinct regions of the IPL termed sublamina. Figure 1.1 shows ON bipolar cell axons stratifying in the sublamina closest to the RGC layer while OFF bipolar cell axons stratify in the sublamina closest to the INL cell bodies. These regions are referred to as the ON and OFF sublamina, or sublamina b and a, of the IPL.

The divergence of cellular processes with regard to ON-OFF pathways is maintained anatomically at the level of RGC dendrites (Famiglietti and Kolb, 1976; Nelson et al., 1978). Dendrites of RGCs that respond to light increments (ON-type RGCs) ramify in the ON (b) sublamina of the IPL while dendrites of RGCs that depolarize to light decrements stratify in the OFF (a) sublamina. Amacrine cell axons also stratify throughout the levels of the IPL in which they respond to light (Freed et al., 1996) with the exception of the dopaminergic amacrine cell (Witkovsky, 2004) (discussed below). The light microscope is a useful tool for

study of the retina due to the lamination of the ON and OFF pathways in the IPL. ON and OFF responses in RGCs are segregated through the lateral geniculate nucleus (Bishop, 1984) and the visual cortex (Hubel and Wiesel, 1962).

Rod and cone photoreceptors are not essential for non-image forming behaviors in mammals.

Non-image forming behavioral responses including entrainment of circadian wheel running behavior and pupil constriction were long thought to be regulated by the rod and/or cone photoreceptor pathway(s) mediating image-forming visual perception. However, several studies have shown that non-image forming behaviors are preserved in mice lacking functional rod and cone photoreceptors (Ebihara and Tsuji, 1980; Foster et al., 1991; Provencio et al., 1998a; Lucas et al., 1999). Similar results have been reported in the photoreceptor deficient Royal College of Surgeons (RCS) rat (Sakamoto et al., 2004) and in the virtually blind mole-rat (David-Gray et al., 1999; Hannibal et al., 2002a; Avivi et al., 2004). Light-induced inhibition of melatonin secretion has been used to study the integrity of the non-image forming visual system in humans. Czeisler and colleagues (1995) have reported that in some visually blind humans, light-induced melatonin suppression is observed and is similar to that of humans with intact rods and cones. In visually blind humans that lack functional rod and/or cone photoreceptors, a small subset of ganglion cell axons form the optic nerve (Cursiefen et al., 2001; Klerman et al., 2002) and may project to non-image forming brain nuclei.

The retinal afferents associated with the non-image forming visual system have been extensively investigated in animal models. The afferents project to a variety of targets including the suprachiasmatic nucleus (SCN) (Moore and Lenn, 1972; Pickard, 1980; Johnson et al, 1988; Pu, 1999), anterior and lateral hypothalamic nuclei (Johnson et al., 1988), the subparaventricular zone (sPVZ) (Pickard and Silverman, 1981;Johnson et al., 1988; Costa et al., 1999), and the ventral lateral preoptic nucleus (VLPO) (Lu et al, 1999). Axons projecting to the SCN also bifurcate and innervate the intergeniculate leaflet (IGL) of the thalamus in hamster (Pickard, 1985). The olivary pretectal nucleus (OPN) is also innervated by non-image forming RGC (Young and Lund, 1998).

The mammalian retina was recently reexamined for the sensory cell(s): rods, cones and other possible retinal neurons accounting for non-image forming visual functions. To discover the cell(s) responsible for sensing light for non-image forming behaviors, Garcia-Fernandez et al. (1995) and Jimenez et al. (1996) reevaluated the temporal pattern of photoreceptor loss in a mouse with inherited photoreceptor degeneration, called the *retinal degenerate* (*rd*) mouse. The *rd* mouse retina contains a small subset of cone photoreceptors that were still present even at 1- and 2-years of age (Carter-Dawson et al., 1978). However, the peak sensitivity of circadian wheel running and pupil constriction (~480 nm) suggests a possible regulatory role of a novel opsin based photopigment (Provencio and Foster, 1995; von Schantz et al., 1997; Lucas et al., 2001; Rea et al., 2001).

In adult mice mutant for rd combined with transgenic ablation of cone photoreceptors fail to possess any functional rod or cone photoreceptors at all. Nevertheless, rd/rd; cl/cl mice do exhibit non-image forming behaviors (Freedman et al, 1999; Lucas and Foster, 1999; Lucas et al., 2001; Mrosovsky et al., 2001; Thapan et al., 2001). Also, transgenic knockout mice lacking mGluR6 glutamatergic receptors on bipolar cells showed abnormal non-image forming behaviors, including an attenuated pupillary light reflex at low light levels (Iwakabe et al., 1997) as well as abnormal masking responses (Takao et al., 2000). More recently, Barnard et al. (2004) used a transgenic mouse in which rods and cones lack the ability to integrate a light stimulus. These animals displayed normal non-image forming behaviors with the exception of an abnormal heart-rate increase after light stimulation (Barnard et al., 2004). Collectively, these data suggest that rod and cone photoreceptors may play an important role in some but not all non-image forming functions. The hypothesis that another non-rod or cone light responsive cell is sufficient for mediating non-image forming behaviors lead to the discovery of a novel photoreceptor within the retina.

The discovery of a third photosensitive neuron in the mammalian retina

Several novel classes of opsin protein have been identified in non-mammalian species, including periopsin (Bellingham et al., 2003), vertebrate ancient opsin (Jenkins et al., 2003), and melanopsin (Provencio et al., 1998b; 2000; Rollag et al, 2000). Melanopsin is the only non-classical-photoreceptor opsin protein expressed in the mammalian retina (for review see Kumbalasiri and

Provencio, 2005). This light-sensitive pigment has been identified specifically in a small subset of RGCs in mice (Provencio et al., 2002a), rat (Hattar et al., 2002), hamster (Bergstrom et al., 2003; Morin et al., 2003; Sollars et al., 2003), non-human primates (Dacey et al., 2005; Jusuf et al., 2007), and humans (Hannibal et al., 2004). Recent studies have shown that melanopsin-containing RGCs project to the SCN (Gooley et al., 2001; Hattar et al., 2002; Sollars et al., 2003) IGL, OPN, sPVZ, VLPO and the superior colliculus (Gooley et al., 2003; Morin et al., 2003; Baver et al., 2008), as well as to the dorsal lateral geniculate nucleus in some species (Dacey et al., 2004; Hattar et al., 2009).

Using an electrophysiological approach, Berson and coworkers (2002) elegantly demonstrated that RGCs projecting to the SCN respond to light without input from the outer retina. Injection of the SCN with a retrograde tracer was used to label afferent RGCs. Labeled RGCs were subsequently blocked pharmacologically from all transmission from rod and/or cone photoreceptors pharmacologically. On light stimulation, these cells still fired action potentials. Critically, when SCN projecting RGCs were physically 'removed' from all retinal input they still responded to light (Berson et al., 2002). These intrinsically photosensitive RGCs (ipRGCs) were shown to contain melanopsin (Berson et al., 2002; Hattar et al., 2002; Sekeran et al., 2003; Semo et al., 2003; Qui et al., 2005; Melyan et al., 2005; Panda et al., 2005; Hartwick et al., 2007). However, their phototransduction mechanism differs from rods and cones in that they depolarize in response to light stimulation (Berson et al., 2002), suggesting that the signal transduction mechanism is more similar to that of invertebrate photoreceptors

(Provencio et al., 1998, Isoldi et al., 2005; Fu et al., 2005; Koyanagi et al., 2005; Hartwick et al., 2007).

Investigation of the role of melanopsin in non-image forming visual function is not fully resolved. Knockout mice lacking the melanopsin gene fail to show masking responses (Mrosovsky et al., 2003), but do not exhibit a complete attenuation of entrainment of circadian rhythms (Panda et al., 2002; Ruby et al., 2002) or the pupillary light reflex (Lucas et al., 2003). However, mice that lack both functional rods/cones and melanopsin show an absence of non-image forming behaviors, including photic entrainment of circadian rhythms and the pupillary light reflex (Hattar et al., 2003). These results indicate both classical photoreceptors and ipRGCs convey light cues to non-image forming visual brain centers.

ipRGCs receive input from rod and cone photoreceptor pathways.

While melanopsin-containing RGCs are intrinsically photosensitive, they nevertheless appear to adhere to classical organizational schemes of the vertebrate retina. In mouse and primates, dendrites of ipRGCs project into different sublamina of the IPL, similar to conventional RGCs (discussed below) (Provencio et al., 2002; Belenky et al., 2003; Dacey et al., 2005). ipRGCs are postsynaptic to amacrine and bipolar cells (Belenky et al., 2003; Dacey et al., 2005; Østergaard et al., 2007; Vugler et al., 2007). However, ipRGCs that ramify in the OFF sublamina of the IPL paradoxically display ON pathway driven responses that are not attributable to a melanopsin phototransduction (Dacey et

al., 2005). Similar results have been obtained in rat (Wong et al., 2007), mouse (Pickard et al., 2009) and rabbit (Hoshi et al., 2009). It therefore does not appear that ipRGCs maintain strict physiological differentiation of ON and OFF pathways as reported for conventional RGCs. The mechanisms of ON input to ipRGCs are not understood. Furthermore, the extent to which rod/cone pathway interneuron(s) contact ipRGCs is not completely known. ipRGCs comprise most if not all of the SCN afferents in mouse (Baver et al., 2008; Güler et al., 2008), suggesting that rod/cone signaling to the circadian clock is primarily through ipRGCs. Thus, illumination signals to non-image forming visual targets are from traditional rod and/ or cone pathway(s), melanopsin responses or a combination of these two photoreceptor systems. It is therefore essential to understand all of the rod and/or cone pathways converging upon ipRGCs.

Classical rod and cone photoreceptor pathways have also been implicated in regulating melanopsin expression levels (i.e. RNA and protein) in ipRGCs. The RCS dystrophic rat is a model for inherited retinal degeneration, which occurs by adulthood (Dowling and Sidman, 1962). The level of melanopsin mRNA is also decreased in photoreceptor degenerate rats compared to animals possessing intact photoreceptors (Sakamoto et al., 2004). However, melanopsin protein expression in ipRGCs does not appear to be altered until after retinal degeneration (Vugler et al, 2007).

There are different ipRGC types in the mammalian retina.

As noted above, melanopsin mRNA expression was originally reported in the mammalian RGC and inner nuclear layers (Provencio et al., 2000) and the first published immunohistochemical evidence of ipRGCs was performed in rat by Hannibal et al. (2002b). Hannibal et al. (2002b) noted that melanopsin immunoreactivity was seen in the cell body, axons and dendrites. This labeling technique has allowed several groups to use melanopsin-immunohistochemistry to independently examine dendrite ramification of ipRGCs (Berson et al., 2002; Hattar et al., 2002). Initial reports using antisera directed against either the amino- or carboxyl- terminus of the rat melanopsin protein suggested that ipRGC dendrites ramify predominantly in the OFF sublamina of the IPL. These results were similar in both rat and mouse retinas using either antiserum (Hattar et al., 2002).

Provencio and colleagues (2002a) generated an antiserum directed against the amino-terminus of the mouse melanopsin protein that unexpectedly contradicted the results of Hattar et al. (2002). Specifically, melanopsin immunoreactive dendrites were observed in the ON sublamina of the IPL, an area which was not detected using the antiserum directed against the amino or carboxyl-terminus of the rat melanopsin protein reported by Hattar and colleagues (2002). There were also twice as many ipRGCs labeled in mouse retinas immunoreacted with the amino-terminus melanopsin antiserum (~1500-1800 melanopsin- immunoreactive RGCs) compared to the antisera generated by Hattar et al. (2002) (~600-800 melanopsin-immunoreactive RGCs) (Hattar et al.,

2002, 2006; Baver et al., 2004). The discrepancy between the total numbers of ipRGCs labeled with the different antibodies is thought to be due to the sensitivity of antibodies (Hattar et al., 2006).

Another intriguing possibility was that there were at least two distinct types of ipRGC in the mouse retina. Conventional RGCs have been segregated morphologically into different types in a number of species including monkey (Perry et al., 1984; Rodieck and Watanabe, 1993; Dacey et al., 2003), cat (Boycott and Wässle, 1974; Stone and Clarke, 1980) rabbit (Amthor et al., 1983), rat (Perry, 1979; Sun et al., 2002a) and mouse (Doi et al, 1995; Sun et al., 2002b; Coombs et al. 2006). The parameters used to classify RGCs into distinct types include size of cell soma and dendrite parameters such as number of primary dendrites, number of dendrite branch points and dendrite ramification in the IPL. In rodent retinas, large scale differences between soma sizes and dendrite parameters are not as evident compared as in primate and cat retinas (Doi et al., 1995; Sun et al., 2002 a,b; Coombs et al., 2006) making dendrite ramification in the ON and OFF sublamina of the IPL an important morphological criterion for cell type determination.

Provencio et al. (2002a), using a new amino-terminus melanopsin antiserum, classified an intricate 'meshwork' of dendrites. However, the complex 'meshwork' of ipRGC immunoreactive dendrites, which is optimal for photon capture for signaling non-image forming visual brain centers, renders anatomical interpretation rather difficult. It is therefore important to circumvent this issue to discriminate ipRGC types in the mouse retina. Using a mouse in which the

tau-lacZ fusion gene is inserted into one mouse melanopsin gene (*tau-lacZ*$^{+/-}$) to produce the protein product β-galactosidase in place of melanopsin (Hattar et al., 2002, 2006) our lab has been able to classify ipRGCs using double labeling immunohistochemistry techniques.

The tau-lacZ homozygous mouse (*tau-lacZ*$^{+/+}$) is a melanopsin knockout mouse (*Opn4*$^{-/-}$) developed by Hattar et al. (2002), which was used to study 1) the role of melanopsin in non-image forming behaviors (Hattar et al., 2003; Lucas et al., 2003) and 2) what brain areas are innervated by ipRGCs (Hattar et al., 2002, 2006). The pupillary light reflex is incomplete at high irradiances in the *tau-lacZ*$^{+/+}$ mouse (Lucas et al., 2003). It is also possible to label ipRGCs that lack melanopsin using antibodies directed against the product of lacZ, which is β-galactosidase (Hattar et al., 2002). The *tau-lacZ*$^{+/-}$ (*Opn4*$^{+/-}$) mouse contains both melanopsin and β-galactosidase (Hattar et al., 2002). The pupillary light reflex (Lucas et al., 2003; Hattar et al., 2003) and entrainment to a 12 h light/ 12 h dark cycle (Hattar et al., 2003) appear to be normal in *tau-lacZ*$^{+/-}$ mice compared to wild-type littermates. However, it is not known whether one copy of β-galactosidase decreases the intrinsic response of ipRGCs.

The *tau-lacZ* mouse (*tau-lacZ*$^{+/+}$; *tau-lacZ*$^{+/-}$) retina contains ~600-800 β-galactosidase-immunoreactive ipRGCs, similar to the number observed with the carboxyl-terminus melanospin antiserum (Hattar et al., 2002, 2006). In chapter 2 we show that ~100% of ipRGCs labeled with the carboxyl-terminus melanopsin antiserum also contain β-galactosidase. These antisera identify approximately half of the immunoreactive ipRGCs identified observed when using the

amino-terminus mouse melanopsin antiserum. To distinguish these subsets of ipRGCs, we named them M1 or M2, depending on whether the cell expresses the tau-lacZ transgene or not. ipRGCs that contain β-galactosidase, termed M1s, comprise 80% of the retinohypothalamic tract (RHT) while ipRGCs that are β-galactosidase negative, termed M2s, comprise 20% of the retinohypothalamic tract (RHT). Thus, ipRGCs comprise the entire extent of the retinohypothalamic tract. Melanopsin and non-melanopsin RGCs project to the OPN. M1s constitute ~45% of the total proportion of those ipRGCs while ~55% are M2s.

The above data (discussed in Chapter 2) used different criteria to differentiate between different ipRGC types compared to conventional RGC type discrimination mentioned previously. Schmidt et al. (2008) generated a mouse in which green fluorescent protein (GFP) is expressed under the control of the melanopsin promoter. This makes it possible to visualize ipRGCs *in vitro* in wholemount retinas. Intracellular injection of Lucifer yellow into GFP expressing ipRGCs led to the identification of three distinct morphological cell types confirming previous results of Warren et al. (2003) in the rat. M1 ipRGC dendrites ramify in the OFF sublamina of the IPL, M2 ipRGC dendrites are confined to the ON sublamina of the IPL while M3 ipRGC dendrites are bistratified in of the ON and OFF sublamina of the IPL (Warren et al., 2003; Schmidt et al., 2008; Schmidt and Kofuji, 2009). Using the immunohistochemical protocol in Baver et al. (2008), GFP-expressing ipRGCs (M1s) ramify strictly in the OFF sublamina of the IPL and GFP-lacking ipRGCs (M2s) appear to be ramifying in the ON sublamina. This

result is consistent with the data published previously in the *tau lacZ* mouse (Baver et al., 2008).

M2 ipRGCs have different light response characteristics than M1 ipRGCs. M2 ipRGCs have a longer latency response to light and lower maximal light response compared to M1 ipRGCs (Schmidt and Kofuji, 2009) and these results have independently been reproduced by Hattar and colleagues (2009). These results are also consistent with differential calcium responses to light stimulation in M1 and M2 ipRGCs (Boldogkoi et al., 2009). These reports are consistent with the suggestion that there are differing levels of melanopsin protein contributing to differential response characteristics between M1s and M2s. It was originally suggested that M2 ipRGCs appear to express less protein based on staining intensity differences between M1 (dark) and M2 (light) ipRGCs (Provencio et al., 2002b; Hattar et al., 2006). There is no current technique available to determine whether there exists differential melanopsin protein expression in M1s compared to M2s ipRGCs.

It is important to determine what factors (e.g. effect of light or outer retinal regulation) regulate melanopsin expression. As noted above, rod and cone photoreceptor pathways regulate melanopsin mRNA in rat (Sakamoto et al., 2004, 2005; Wan et al., 2006). It is therefore possible that ON and OFF bipolar/ amacrine cells regulate melanopsin RNA/protein expression in ipRGCs, explaining the differential protein levels reported in mouse ipRGC types. The developing mouse retina could be used as model to understand how outer retinal development affects melanopsin protein regulation. Using two independent

transgenic mouse lines, I show that at birth ipRGCs are not differentiated into different cell types. By postnatal day (PD) 10, the evidence for two types of ipRGC in both transgenic mouse lines becomes increasingly apparent. At birth, conventional RGC dendrites ramify throughout the entire extent of the IPL. In the adult mouse, approximately 75% of conventional RGC dendrites 'monostratify' either in the ON or OFF sublamina of the IPL while the remaining RGCs are bistratified (Coombs et al. 2006). Furthermore, rod/cone photoreception is critical for proper RGC development (Bodenarko et al., 1999; Tian and Copenhagen, 2003, Tian, 2008). Consistent with conventional RGC development, ipRGC differentiation is regulated by light. Dopamine also plays an important role in melanopsin expression regulation in rat (Sakamoto et al., 2005). In the final set of experiments in Chapter 3, I sought to determine the role of dopamine on ipRGC development and suggest that dopamine transmission also plays an important role in ipRGC type development.

In summary, I have developed a novel and reproducible technique to distiniguish two types of ipRGC in the mouse retina, termed the M1 and M2 ipRGCs. These types differentially innervate visual brain centers involved in circadian entrainment and pupillary light reflex. ipRGCs develop in a manner similar to that of conventional RGCs as well as rely on input from the outer retina for regulation of melanopsin expression. Taken together, my findings suggest there may be an intricate communication between the outer retina and ipRGCs that allows for the entire dynamic range of light intensities to be signaled in the brain for non-image forming visual processing.

Chapter 2

Two types of melanopsin retinal ganglion cell differentially innervate the hypothalamic suprachiasmatic nucleus and olivary pretectal nucleus

Abstract

Melanopsin-expressing intrinsically photosensitive retinal ganglion cells (ipRGCs) innervate the hypothalamic suprachiasmatic nucleus (SCN) and the olivary pretectal nucleus (OPN) providing irradiance information for entrainment of circadian rhythms and for stimulating the pupillary light reflex. In this study, mice were used in which the melanopsin gene was replaced with the *tau-lacZ* gene. Heterozygous (*tau-lacZ*$^{+/-}$) mice express both melanopsin and β-galactosidase. In *tau-lacZ*$^{+/-}$ mice, only ≈ 50% of ipRGCs contain β-galactosidase and these cells are specifically labeled with a C-terminus melanopsin antibody. Retrograde tracer injection into the SCN labels β-galactosidase-expressing ipRGCs (termed M1) that comprise ≈ 80% of the SCN-projecting ipRGCs. M1 ipRGCs and an additional set of ipRGCs (termed M2) are labeled with a melanopsin antiserum targeted against the N-terminus of the melanopsin protein; M2 ipRGCs do not contain detectable β-galactosidase and these cells make up the remainder of the SCN-projecting RGCs. Tracer injection into the OPN labeled non-melanopsin RGCs and both types of ipRGC: 45% M1 and 55% M2. The two subtypes of ipRGCs project differentially to the SCN and OPN the functional significance of ipRGCs subtypes is currently unknown.

Introduction

Melanopsin-containing retinal ganglion cells are intrinsically photosensitive (ipRGCs) (Berson et al., 2002; Warren et al., 2003; Sekaran et al., 2003; Hartwick et al., 2007) and provide irradiance signals to several central targets including the hypothalamic suprachiasmatic nucleus (SCN) and the olivary pretectal nucleus (OPN). Retinal input to the hypothalamus entrains the SCN circadian clock to the day/night cycle (Moore and Lenn, 1972; Pickard, 1982); retinal fibers terminating in the OPN provide the afferent limb of the pupillary light reflex (Trejo and Cicerone, 1984; Clarke and Ikeda, 1985). ipRGC input to the SCN and OPN has been described in rodents using retrograde tracers coupled with identification of ipRGCs either by *in situ* hybridization for melanopsin mRNA (Gooley et al., 2003) or with immunohistochemical techniques (Hattar et al., 2002; Morin et al., 2003; Sollars et al., 2003). In addition, ipRGC axonal distribution to the SCN and OPN has been demonstrated using a knock-in mouse model in which the *tau-lacZ* gene replaces the melanopsin *opn4* gene (Hattar et al., 2002, 2006). Immunohistochemical visualization of the β-galactosidase reporter protein indicates a projection to the SCN that arises predominately from ipRGCs. The melanopsin terminal field in the OPN identified through this method is restricted to the periphery or shell of the nucleus although retinal input to the entire rodent OPN (i.e. peripheral shell and central core) is well documented (Scalia, 1972; Scalia and Arango, 1979; Pak et al., 1987).

However, it appears that for unknown reasons the number of ipRGCs expressing β-galactosidase in the retina of the heterozygous *tau-lacZ*$^{+/-}$ mouse (600-800 cells) represents only about one half of the 1200 -1600 ipRGCs in the retina (Lucas et al., 2003; Hattar et al., 2006). Presumably the level of β-galactosidase expressed in the remaining half is undetectable by immunohistochemical procedures (Hattar et al., 2006). Moreover, the ipRGCs that express β-galactosidase in the *tau-lacZ* mouse appear to be a specific subset of ipRGCs (termed M1). The rationale for subdividing ipRGCs into groups is based on immunohistochemical and morphological criteria: 1) M1 cells stain more heavily with a sensitive melanopsin antibody (UF006; Provencio et al., 2002) suggesting a greater level of protein; 2) M1 cells are slightly smaller and have more dendrites than the other subset of ipRGCs (termed M2) (I. Provencio, personal communication); and 3) the dendrites of M1 ipRGCs appear to terminate in the outermost tier of the inner plexiform layer (IPL) whereas M2 dendrites may be confined to the proximal IPL (see Hattar et al., 2006). Thus, if M2 ipRGCs are a separate subset of ipRGCs and they do not express β-galactosidase in the *tau-lacZ*$^{+/-}$ knock-in mouse, their central projections are currently unknown. In this study we investigated the projections of ipRGCs in the *tau-lacZ*$^{+/-}$ mouse using retrograde tracers together with immunohistochemical procedures for β-galactosidase and two different melanopsin antibodies.

Materials and Methods

Animals

Mice of a mixed B6/129 strain (10-12 weeks old) genetically modified to generate a tau-lacZ$^{+/-}$ protein in place of the melanopsin protein (Hattar et al., 2002, 2006; Lucas et al., 2003) were used in this study as well as wild-type mice of similar age (C57BL/6J, Jackson Laboratory, Bar Harbor, ME). The *tau-lacZ* knock-in mice were raised in our laboratory from mice generously supplied by Dr. Samer Hattar (Johns Hopkins University). Animals were maintained under a 12 h light/12 h dark cycle with lights on at 0700, with food and water available *ad libitum*. Animals were killed between 1000 and 1400 h. All experiments were performed according to the National Institutes of Health guidelines for the Care and Use of Laboratory Animals and were approved by the Colorado State University Animal Care and Use Committee.

Retrograde Labeling

To retrogradely label retinal ganglion cells projecting to the SCN or OPN, mice were anesthetized by isoflurane (2.5-5%) inhalation anesthesia and placed in a Kopf stereotaxic holder. A craniotomy was performed above the injection site (SCN: -0.5 AP, -5.6 DV, 1.25 ML; OPN: -2.5 AP, -1.9 DV, 1.0 ML) and a glass micropipette attached to a Nanoject II (Drummond Scientific Co, Broomall, PA) was used to deliver tracer. The tracer injected was 207 nl of either a recombinant strain of pseudorabies virus (PRV152) constructed to express enhanced green fluorescent protein (EGFP; Smith et al., 2000) (1 X 10^8 pfu/ml) (SCN injections) or

cholera toxin-β subunit conjugated to Alexa Fluor 594 (Molecular Probes, Eugene, OR) (OPN injections - 5 μg/μl in 0.9% saline and 2% DMSO). The glass micropipette was left in place for about 1 minute after tracer delivery before being slowly retracted.

Forty-eight hours post-injection, animals were deeply anesthetized with sodium pentobarbital (80 mg/kg, i.p.) and perfused transcardially with 0.9% saline followed by cold freshly prepared fixative consisting of 4% paraformaldehyde in 0.1 M phosphate buffer (pH 7.3). Eyes were enucleated, anterior segments and vitreous were removed and eyecups were embedded in 7% gelatin (100 bloom, Fisher Scientific) and placed in the same fixative with 20% sucrose overnight at 4 °C. Eyecups were sectioned at 40 μm on a sliding microtome equipped with a freezing stage (Physitemp Instruments Inc., Clifton, NJ) and sections were collected in phosphate buffered saline (PBS).

Immunohistochemistry

Light microscopic immunohistochemistry was performed on free-floating sections. After rinsing in PBS, sections were transferred to a blocking solution in PBS containing 4% normal goat serum (NGS, Sigma), 0.4% triton X-100 (TX, Sigma) and 1% bovine serum albumin (BSA) and were then transferred to the primary antiserum: either rabbit anti-melanopsin N-terminus antibody diluted 1:5000 (UF006 generously provided by Ignacio Provencio) (Provencio et al., 2002), rabbit anti-melanopsin C-terminus antibody diluted 1:500, (#PA1-781, Affinity BioReagents, Golden, CO), or chicken anti-β-galactosidase antibody

diluted 1:500 (ab9361, Abcam, Cambridge, MA) containing 1% NGS, 0.4% TX in 1% BSA for 24 h at room temperature (rt). Primary antisera were visualized with either a goat anti-rabbit IgG or goat anti-chicken IgY conjugated either to Alexa Fluor 488 or Alexa Fluor 594 (Molecular Probes) diluted 1:400 in PBS for 60 minutes (rt). Sections were rinsed in PBS, mounted on subbed slides, coverslipped with Vectashield (Vector Laboratories, Burlingame, CA) and sealed with fingernail polish to prevent dehydration. Double labeling with the rabbit and chicken primary antibodies was performed concurrently and controls in which one primary antibody was omitted revealed no cross reactivity between the goat secondary antibodies generated against rabbit IgG or chicken IgY. Specificity of both the C-terminus and N-terminus melanopsin antibodies was evaluated by staining retinas from *tau-lacZ*$^{+/+}$ mice in which both *opn4* genes had been replaced with the tau-lacZ gene; no immunopositive cells were observed in the *opn4* knockout mice (data not shown).

Double labeling with the C-terminus and N-terminus rabbit anti-melanopsin antisera was performed using direct labeling of the UF006 N-terminus antiserum with Alexa Fluor 594. Because direct conjugation of Alexa Fluor 594 to the primary antibody is less efficient than labeling with a secondary antibody, a high titer antibody is required and therefore the UF006 antibody was chosen for the Alexa Fluor 594 conjugation. Sections were initially processed for the C-terminus melanopsin antisera using a goat anti-rabbit Alexa Fluor 488 secondary antibody as described above. Sections were then rinsed in PBS (3 X 15 min) and incubated in PBS containing 3% NGS, 0.4% TX, rabbit anti-lucifer yellow (1:200; any rabbit

IgG that is generated against an antigen not found in the native tissue can be used here) and 1% BSA for 1 h (rt). After further rinsing (3 X 15 min), sections were blocked in donkey anti-rabbit Fab (Jackson Immunoresearch, West Grove, PA), rinsed (3 X 15 min) and incubated (2 h, rt) in the N-terminus melanopsin antibody directly conjugated to Alexa Flour 594 using a Zenon kit as described by the manufacturer (Molecular Probes). Sections were rinsed (2 X 10 min) followed by incubation in 4% paraformaldehyde in PBS (15 min), wash (3 X 10 min) and then mounted on subbed slides, coverslipped with Vectashield and sealed. When a non-melanopsin rabbit IgG was substituted for rabbit anti-N terminus antibody and processed using the Zenon direct conjugation kit as described above, no Alexa Fluor 594 label was observed indicating that the initial goat anti-rabbit IgG secondary was bound and/or blocked and therefore did not cross-react with the second rabbit primary antibody conjugated to Alexa Fluor 594.

Sections were first examined for one label (e.g., Alexa Fluor 488 using EGFP optics; #41020 High Q narrow band EGFP filter; Chroma, Brattleboro, VT) and then the other label (e.g., Alexa Fluor 594 using Texas Red optics; #41004 HQ Texas Red filter, Chroma) with final confirmation of the analysis by examining both red and green signals concurrently using a dual band filter (#51019 Texas Red/EGFP, Chroma). Background staining was low and it was straightforward to determine positively labeled cells. Compilation of the percentage of double-labeled cells was performed only after all tissue from each experiment had been analyzed. The numbers of retinal sections analyzed varied from case to

case as sections were lost or damaged during the double-label procedures. For the analysis contributing data to Table 2.1, all immunolabeled cells in each section analyzed were counted. For the analysis contributing data to Table 2.2, all PRV152 labeled cells in each section analyzed were counted. Only immunolabeled cells that were also PRV152 labeled were counted. Thus, the many immunolabeled RGCs whose central projections were undetermined (i.e., not PRV152 labeled) were not included. For the analysis contributing data to Table 2.3, all immunolabeled cells were counted in the retina contralateral to the injection and the number of cells also labeled with CTB was determined. Cells labeled only with CTB were not included in the analysis.

Slides were examined using a Leica (Nussloch, Germany) DMRA light microscope equipped with epifluorescence and fitted with a microstepping servomotor in the z–axis. Images were captured using a Hamamatsu (Hamamatsu City, Japan) C4742-95 CCD digital camera under epifluorescence and deconvolved using Openlab fluorescence deconvolution software (Improvision, Boston, MA) running on an Apple Macintosh G-4 platform. Digital images were pseudo-colored, and images were prepared using Adobe Photoshop version 6.0.1. Images were enhanced for brightness and/or contrast.

Results

Two types of melanopsin RGC

In retinas from *tau-lacZ*$^{+/-}$ mice, β-galactosidase immunofluorescence was observed in cells primarily in the ganglion cell layer with an occasional cell also labeled in the inner nuclear layer as described previously (Hattar et al., 2002) (Figure 2.1a). Double-labeling using a chicken anti-β-galactosidase antibody with a rabbit anti-melanopsin antibody (UF006) generated against the 15 N-terminus amino acid sequence of the predicted mouse melanopsin protein (Provencio et al., 2002), confirmed that the β-galactosidase reporter enzyme was expressed in ipRGCs (Hattar et al., 2002); all β-galactosidase immunopositive cells were also melanopsin immunopositive (Figure 2.1a-c). However, only about one half of the N-terminus melanopsin-labeled RGCs examined in sections from both retinas of three *tau-lacZ*$^{+/-}$ mice were β-galactosidase-positive; from a total of 1426 N-terminus melanopsin-labeled cells observed, 803 were also β-galactosidase immunopositive (56.3%; Table 2.1) (Figure 2.1a-c). When a similar double label analysis was conducted on retinal sections from the same three *tau-lacZ*$^{+/-}$ mice using a C-terminus melanopsin antibody raised against the 20 C-terminus amino acid sequence of the predicted rat melanopsin protein (Affinity BioReagents), almost all β-galactosidase-labeled RGCs were melanopsin-positive. From a total of 654 β-galactosidase immunopositive cells observed, 604 were also C-terminus immunopositive (92.4%; Table 2.1) (Figure 2.1d-f), a finding significantly different from the results observed after double labeling with β-galactosidase and the N-terminus melanopsin antibody ($p < 0.00001$, Fisher's exact test).

The distribution of melanopsin dendritic processes in the IPL also appeared different in the C-terminus labeled retinas. Whereas two distinct plexuses of melanopsin processes were evident in the IPL of the N-terminus stained retinas (Figure 2.1b), the processes in the IPL along the border of the ganglion cell layer appear to be absent in the C-terminus and β-galactosidase stained material (Figure 2.1d-f). Melanopsin processes are less effectively labeled than melanopsin cell bodies when the N-terminus antibody is directly conjugated to Alexa Fluor 594 and therefore neither plexus is prominent in tissue stained in this manner (Figure 2.1h).

The very high coincidence of β-galactosidase and C-terminus melanopsin labeling suggests that these markers label the same population of RGCs. We thus predicted that double labeling of retinal sections with both the C- and N-terminus rabbit anti-melanopsin antibodies would produce a similar proportion of doubled-labeled cells as observed after β-galactosidase and N-terminus melanopsin labeling (i.e., 56.3%). In 90 retinal sections from a wild-type mouse, 1422 cells were labeled with the N-terminus melanopsin antibody. Of these 1422 cells, 802 were also labeled with the C-terminus antibody (56.3%) (Figure 2.1g-i), similar to the result obtained after double labeling with β-galactosidase and the N-terminus melanopsin antibody in *tau-lacZ*$^{+/-}$ mice.

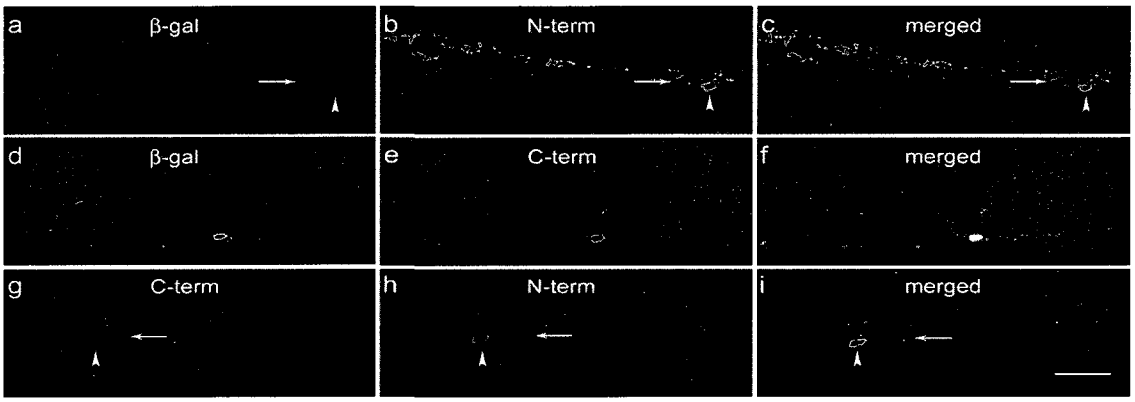

Figure 2.1. Two types of melanopsin retinal ganglion cell. Double-labeled retinal ganglion cells (RGCs) in the *tau-lacZ*$^{+/-}$ mouse retina immunopositive for β-galactosidase (β-gal) (a), N-terminus melanopsin (N-term) (b), and merged image (c). Double-labeled RGCs in the *tau-lacZ*$^{+/-}$ mouse retina immunopositive for β-galactosidase (d), C-terminus melanopsin (C-term) (e), and merged image (f). Double-labeled RGCs in the *tau-lacZ*$^{+/-}$ mouse retina immunopositive for C-terminus melanopsin (g), N-terminus melanopsin (h), and merged image (i). Scale bar = 50 μm. Arrowheads indicate M1s while arrows show M2s.

Moreover, C-terminus melanopsin labeling was only observed in cells also labeled with the well-characterized UF006 N-terminus melanopsin antibody (Provencio et al., 2002; Belenky et al., 2003; Morin et al., 2003), providing additional confirmation of the specificity of the C-terminus antibody. Thus, it appears that in the retina of the *tau-lacZ*$^{+/-}$ knock-in mouse, β-galactosidase is expressed in only about 50% of ipRGCs and these cells, termed M1, are specifically labeled with an antibody generated against the intracellular C-terminus of melanopsin.

	tau-lacZ 1	tau-lacZ 2	tau-lacZ 3	Total
β-gal/	327/	224/	252/	803/
N-term	542	471	413	1426
	60.3%	47.6%	61.0%	56.3%
no. of sections	(34)	(34)	(29)	(97)
C-term/	297/	186/	121/	604/
β-gal	315	201	138	654
	94.3%	92.5%	87.7%	92.4%
no. of sections	(39)	(25)	(14)	(78)
	B6a	B6b	B6c	Total
C-Term/	221/	222/	359/	802/
N-term	398	397	627	1422
	55.5%	55.9%	57.3%	56.4%
no. of sections	(28)	(28)	(34)	(90)

Table 2.1. Two types of melanopsin retinal ganglion cell. Retinal sections from both eyes of three tau-lacZ$^{+/-}$ mice were double labeled for β-galactosidase (β -gal) and melanopsin using N-terminus (N-term) or C-terminus (C-term) antibodies. Two populations of melanopsin-containing retinal ganglion cell (RGC) were observed. Approximately one-half (56%) of melanopsin RGCs labeled with the N-term antibody expressed β-gal whereas almost all RGCs expressing β-gal stained with the C-term antibody (92%). C-term or β-gal staining defines type M1 melanopsin RGCs. N-term labeled cells not expressing β-galactosidase are defined as type M2 RGCs. No RGCs were labeled with either melanopsin antibody in retinal sections from tau-lacZ$^{+/+}$ mice. Two populations of melanopsin-containing RGC were also observed using the N-term and C-term antibodies in three C57/B6 mouse retinas. Approximately one-half (56%) of melanopsin RGCs labeled with the N-term antibody expressed C-term immunoreactivity.

Since one half of the ipRGCs do not express β-galactosidase, their axons are not labeled and consequently the central projections of these cells, termed M2, are unknown. We examined the potential projections of these cells to the SCN and OPN using retrograde tracing techniques.

M1 and M2 melanopsin RGC projections to the SCN

Since β-galactosidase or C-terminus melanopsin immunolabeling are specific markers for M1 ipRGCs in the *tau-lacZ*$^{+/-}$ mouse whereas the N-terminus melanopsin immunolabeling appears to label both the M1 and M2 ipRGCs, we examined the relative proportion of M1 and M2 SCN-projecting ipRGCs in the retinas of *tau-lacZ*$^{+/-}$ mice following retrograde tracer injection into the hypothalamus directed at the SCN (n=5 *tau-lacZ*$^{+/-}$ animals and n=2 wild-type animals).

To avoid labeling axons of the optic chiasm, tracer injections were targeted to the dorsocaudal border of the SCN. In preliminary experiments using rhodamine-labeled microspheres as a retrograde tracer, such injections labeled very few RGCs. Greater success was achieved using the retrograde transsynaptic tracer PRV152 (Pickard et al., 2002), because virus placed at the dorsocaudal border of the SCN was taken up by SCN neuronal processes and transported to the soma of SCN neurons where viral replication occurred resulting in EGFP expression throughout the SCN (Figure 2.2a). After the first round of viral replication, PRV152 transsynaptically infected retinal terminals in the SCN. The

virus was then retrogradely transported to the retina where a second round of viral replication occurred, labeling SCN-projecting ganglion cells with EGFP.

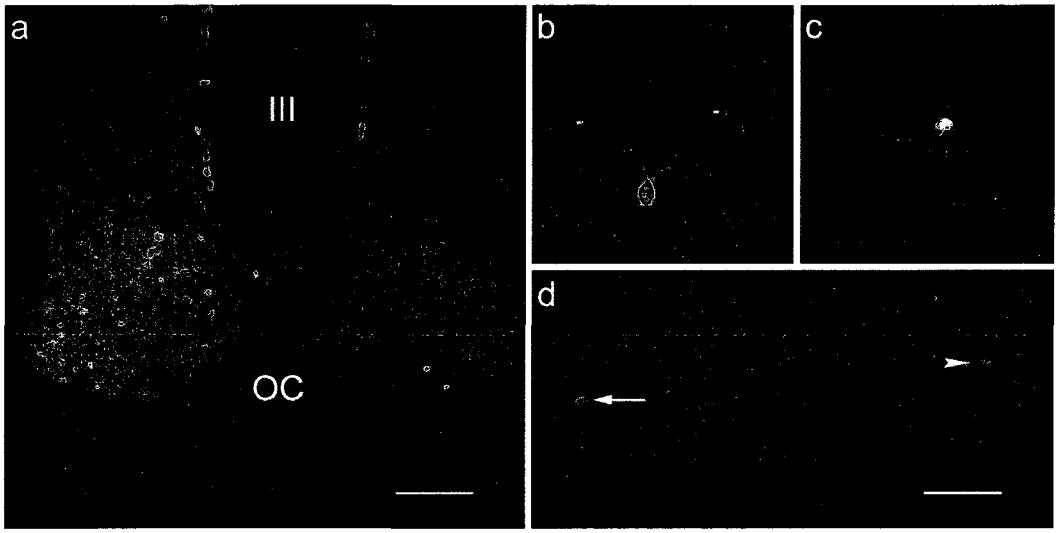

Figure 2.2. Two types of melanopsin retinal ganglion cell innervate the suprachiasmatic nucleus. An EGFP-expressing pseudorabies virus (PRV152) was unilaterally injected into the region of the suprachiasmatic nucleus (SCN) resulting in expression of EGFP in the SCN bilaterally after viral replication (a). After transsynaptic infection of retinal terminals and retrograde transport to both retinas, PRV152 labeled cells in the ganglion cell layer (green) were N-terminus melanopsin immunopositive (red) shown in the merged image (b) and PRV152 labeled displaced retinal ganglion cells (RGCs) in the inner nuclear layer (green) were N-terminus melanopsin immunopositive (red) shown in the merged image (c). About 80% of the PRV152 retrogradely labeled RGCs (green) were β-galactosidase immunopositive (red) shown in the merged image (d). Scale bars: (a) = 100 μm; b-d = 50 μm.

The post-injection survival period of 48 h limited viral replication to just two rounds and no PRV152 labeled amacrine or bipolar cells were observed in the retina. The short post-injection survival period also eliminated neurons in the intergeniculate leaflet (IGL) from contributing to transsynaptic labeling of retinal ganglion cells. IGL neurons are afferent to the SCN (Pickard, 1982) and thus were labeled in these experiments (data not shown). However, for the IGL to contribute to the retrograde label in the retina, a third round of viral replication after transport

from the IGL to the retina would have been necessary (i.e., SCN 1st round of replication → RGC 2nd round of replication vs SCN 1st round of replication → IGL 2nd round of replication → RGC 3rd round of replication).

Immunolabeling of EGFP-labeled retinal sections from five *tau-lacZ*$^{+/-}$ mice and two wild-type mice with the N-terminus melanopsin antibody revealed that virtually all (98.0%) SCN-projecting RGCs were melanopsin-positive; of 893 EGFP-labeled SCN-projecting RGCs observed, 875 were also labeled with N-terminus melanopsin antibody (Table 2.2) (Figure 2.2b&c). Immunolabeling of retinal sections from four *tau-lacZ*$^{+/-}$ mice with the β-galactosidase antibody revealed that only 79.3% of PRV152 labeled SCN-projecting RGCs were double-labeled; of 574 EGFP-labeled RGCs observed, 455 were labeled with the β-galactosidase antibody (Figure 2.2d). Thus, SCN-projecting RGCs in the mouse appear to be comprised almost solely of melanopsin RGCs with the vast majority (80%) of the M1 type and the remaining 20% M2 ipRGCs.

M1 and M2 melanopsin RGC projections to the OPN

To assess the relative proportion of M1 and M2 ipRGCs that project to the OPN, CTB conjugated to Alexa Fluor 594 was used as a retrograde tracer. Injections of CTB directed at the OPN (Figure 2.3a) produced hundreds of retrogradely labeled RGCs in the retina contralateral to the injection (Figure 2.3b). Immunostaining with the C-terminus melanopsin antibody (n=1 animal) or the

	tau-lacZ 11	tau-lacZ 15	tau-lacZ 1	tau-lacZ 2	tau-lacZ 3	B6-1	B6-4	total
N-term/	134/	100/	155/	149/	153/	172/	12/	875/
PRV	135	102	162	154	155	173	12	893
Perc	99.3	98.0	95.6	96.8	98.7	99.4	100	98.0
no. of sect.	(34)	(15)	(27)	(28)	(31)	(36)	(9)	(180)
	tau-lacZ 11	tau-lacZ 15	tau-lacZ 9	tau-lacZ 16	total			
β-gal/	95/	69/	101/	190/	455/			
PRV	114	83	132	245	574			
Perc	83.3	83.1	76.5	77.6	79.3			
no. of sect.	(25)	(12)	(30)	(32)	(99)			

Table 2.2. Two types of melanopsin retinal ganglion cell innervate the suprachiasmatic nucleus. A recombinant of the Bartha strain of pseudorabies virus (PRV) expressing EGFP (PRV152) was injected into the SCN region to retrogradely label retinal ganglion cells (RGCs) in seven tau-lacZ$^{+/-}$ mice and two wild-type mice (B6). Virtually all SCN-projecting RGCs labeled with PRV in two tau-lacZ$^{+/-}$ mice and two wild-type mice were melanopsin-containing RGCs (98%). Approximately 80% of melanopsin RGCs projecting to the SCN (i.e., PRV-labeled in four tau-lacZ$^{+/-}$ mice) were labeled with β-gal antibody and are defined as M1 type RGCs.

β-galactosidase antibody (n=2 animals) to specifically label M1 cells revealed that approximately 60% of the C-terminus melanopsin/β-galactosidase labeled RGCs were also labeled with CTB; of 349 immunolabeled RGCs noted, 204 were

labeled with CTB (58.4%, Table 2.3) (Figure 2.3b). Since all of the M1 ipRGCs would also have been labeled by the N-terminus antibody, it follows that 58.4% * 56% = 33% of the N-terminus labeled cells would have been expected to be double labeled with the CTB. Many more (i.e., 621 N-terminus) RGCs were doubled labeled with CTB from a total of 846 N-terminus labeled cells observed (73.4%, Table 2.3). Thus, we found that 40% (73% minus 33%) of the entire population of ipRGCs was both type M2 and OPN-projecting, whereas 33% were type M1 OPN-projecting cells. Hence, of the melanopsin labeled ipRGCs projecting to the OPN, 45% (33%/73%) were of type M1, and 55% [(73%-33%)/73%] were of type M2.

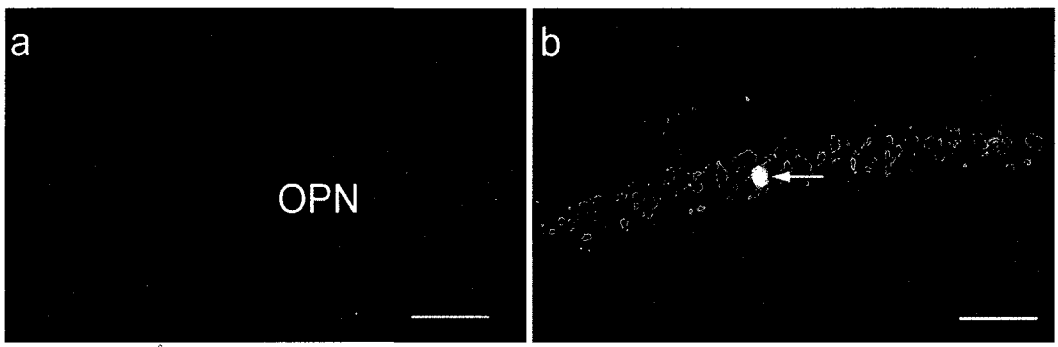

Figure 2.3. Two types of melanopsin retinal ganglion cell innervate the olivary pretectal nucleus. Cholera toxin-β subunit conjugated to Alexa Fluor 594 (CTB) was injected into the pretectum aimed at the olivary pretectal nucleus (OPN) (a). CTB was retrogradely transported to the retina and labeled many retinal ganglion cells (RGCs). Approximately 45% of RGCs immunopositive for N-terminus melanopsin were also labeled with CTB (arrow) (b) whereas about 55% of β-galactosidase labeled RGCs were CTB labeled (not shown). Scale bars: (a) = 100 μm; b = 50 μm

The retinas of two mice in which the CTB injections missed the OPN but labeled the superior colliculus (SC) were also examined. In these mice, 26% (22.9% and 29.2% respectively) of the β-galactosidase labeled RGCs were double labeled with CTB (38 double labeled RGCs from a total of 146 immunolabeled cells; Table 2.3), so 26% * 56% = 15% of the N-terminus labeled cells would have been expected to be double labeled with CTB. In contrast with the results from the OPN, approximately 10% of the N-terminus labeled cells were double labeled with CTB (41 of 414 immunolabeled RGCs; Table 2.3). Since all of the β-galactosidase labeled cells would also have been labeled with N-terminus antibody, it follows that 0% of the ipRGCs projecting to the SC would have been labeled by N-terminus but not β-galactosidase antibodies. Hence, 100% of the ipRGCs projecting to the SC were of type M1.

Here, we have established differential innervation of the SCN, OPN, and SC by ipRGCs of type M1 and M2: 80% of the ipRGCs innervating the SCN were of type M1; 45% of the ipRGCs innervating the OPN were of type M1; and 100% of the ipRGCs innervating the SC were of type M1.

	OPN1 * -	OPN-5	OPN8	total	SC-1	SC-2	Total
CTB + β-gal/	49/	68/	87/	204/	17/	21/	38/
β-gal	75	109	165	349	74	72	146
	65.3 %	62.4%	53.0%	58.4%	22.9%	29.2%	26.0%
no. of sec	(13)	(10)	(13)	(36)	(9)	(7)	(16)
CTB + N-ter m/	330/	141/	150/	621	26/	15/	41/
N-ter m	421	190	235	846	232	182	414
	78.4 %	72.4%	63.8%	73.4%	11.2%	8.2%	9.9%
no. of sec	(14)	(13)	(18)	(45)	(8)	(7)	(15)

Table 2.3. M1 and M2 melanopsin retinal ganglion cells innervate the olivary pretectal nucleus. Cholera toxin β-subunit (CTB) conjugated to Alexa Fluor 594 injected into the olivary pretectal nucleus (OPN) or the superior colliculus (SC) in *tau-lacZ*$^{+/-}$ mice produced retrogradely labeled retinal ganglion cells (RGCs) almost exclusively in the retina contralateral to the injection. The contralateral retina was stained for β-galactosidase (β -gal) or C-terminus (C-term) melanopsin (*) or an N-terminus (N-term) melanopsin and double-labeled RGCs were compared to the total number of melanopsin-stained RGCs.

Discussion

The *tau-lacZ*$^{+/-}$ mouse synthesizes β-galactosidase linked to the tau protein that is expressed predominately in the axons of neurons. This mouse model has played an important role in furthering our understanding of the retinofugal projections of melanopsin-expressing ipRGCs and the broad range of target structures innervated by these unique photoreceptive neurons (Hattar et al., 2002; 2006). The principal finding in this study is that only approximately one half of the melanopsin RGCs in this mouse model express β-galactosidase and that these cells are specifically labeled with a melanopsin antibody generated against the C-terminus of the rat melanopsin protein. These ipRGCs, termed M1, and about an equal number of additional ipRGCs, termed M2, are labeled with a melanopsin antibody generated against the N-terminus of the mouse melanopsin protein. Data are also provided in this study showing for the first time that the two different types of ipRGC differentially innervate the SCN, OPN, and SC; the melanopsin input to the SCN is dominated by M1 ipRGCs whereas the majority of the ipRGC input to the OPN is from M2 cells.

It has been suggested that the dendrites of M2 melanopsin cells may be confined to proximal zone to the IPL near the border of the ganglion cell layer (Hattar et al., 2006). The dendrites of ganglion cells stained with either β-galactosidase or the C-terminus melanopsin antibody (M1 cells) appear to stratify in the distal IPL with few if any immunoreactive processes in the proximal IPL. Staining with the N-terminus antibody reveals two bands of melanopsin processes in the IPL, suggesting that M2 cells have dendrites confined primarily

to the proximal IPL. Intracellular filling of ipRGCs to follow the complete arborization of the dendritic processes in the IPL for M1 and M2 cells has been described by Schmidt et al. (2008). Indeed, Schmidt et al. (2008) showed type I dendrites, which correspond to M1 ipRGC dendrites, stratify in the OFF sublamina of the IPL while type II, which correspond to M2 ipRGCs, are confined to the ON sublamina of the IPL (Schmidt et al., 2008).

ipRGC input to the SCN

The RGC input to the mouse SCN is comprised almost entirely, if not completely, of ipRGCs based on the observation in this study that more than 98% of SCN-projecting RGCs were melanopsin-immunopositive. To our knowledge, these are the first quantitative data describing retrogradely labeled ganglion cells in the mouse retina after tracer injection into the SCN. These findings differ somewhat from previous observations in the rat and golden hamster, where it has been estimated that 10-30% of the ganglion cells that innervate the SCN are non-melanopsin RGCs (Gooley et al., 2003; Morin et al., 2003; Sollars et al., 2003). Recent data from Güler et al. (2008) are consistent with our findings in the mouse. These investigators selectively ablated ipRGCs in mice by knocking in diphtheria toxin A (DTA) in the melanopsin locus; elimination of melanopsin RGCs resulted in complete loss of light-induced behavioral responses mediated by the SCN (Güler et al., 2008). Thus, RGC input to the SCN appears to vary from 100% melanopsin RGCs in the mouse to 80-90% ipRGCs in the hamster and perhaps 70% melanopsin RGCs in the rat (Gooley et al., 2003; Morin et al., 2003;

Sollars et al., 2003). In the mouse, the only species in which there are experimental tools to access different types of melanopsin RGC, 80% of the retinohypothalamic tract (RHT) is comprised of M1 ipRGCs and 20% M2 ipRGCs.

If the RHT input to the mouse SCN consists entirely of ipRGCs and both M1 and M2 melanopsin RGCs contribute to the RHT, it would seem reasonable to suggest that both the M1 and M2 RGCs are intrinsically photosensitive. To date, this has not been tested directly (see Hattar et al., 2006) although there is indirect evidence that M2 RGCs in addition to the M1 RGCs in the mouse are intrinsically photosensitive. Using the same UF006 N-terminus melanopsin antibody used in this study that labels M1 and M2 RGCs, we and others have shown that between 70-80% of melanopsin RGCs express Fos in response to light in retinal degenerate mice lacking rods and cones (Semo et al., 2003; Pickard et al, 2009). Since only 50% of the melanopsin RGCs are of the M1 subtype, the observation that 70-80% of melanopsin cells were Fos immunopositive indicates that at least some, if not all, M2 ipRGCs are intrinsically photosensitive as well. Two physiological types of ipRGC have also been reported in the adult mouse retina although it is not clear if these correlate with the M1 and M2 types of melanopsin RGC (Tu et al., 2005). Dacey and co-workers have described two morphological subtypes of ipRGCs in the primate and both are intrinsically photosensitive (Dacey et al., 2005).

ipRGC input to the OPN

The M1 ipRGC projection to the OPN has been described in the *tau-lacZ*$^{+/-}$ mouse as forming a shell surrounding the circular field of overall retinal input (Hattar et al., 2006). The M1 ipRGC terminal zone in the outer shell of the mouse OPN corresponds to the location of OPN projection neurons that innervate the EW in the rat (Smeraski et al., 2004). Using the retrograde tracer CTB we have shown that M2 ipRGCs also innervate the OPN. The ratio of M1 ipRGCs projecting to the OPN is 45% while the 55% of the ipRGCs are M2s. Non-melanopsin RGCs may also innervate the OPN core, consistent with an attenuated but still functional pupillary light reflex in DTA melanopsin ablated mice lacking all ipRGCs (Güler et al., 2008).

In summary, two types of melanopsin-expressing RGC differentially innervate the SCN and OPN, with M1 ipRGCs the predominate type innervating the SCN and M2 ipRGCs comprising the majority ipRGC input to the OPN. M1 and M2 ipRGCs may integrate different signals in the retina with their intrinsic response to light based on the interpretation that their dendrites stratifiy in the OFF and ON layers of the IPL, respectively. Integration of the M1 and M2 inputs may play a role in the overall dynamic range of the responses of the SCN and OPN to retinal irradiance. Future experiments may determine if the signals carried by these two subtypes of ipRGC to their central targets are defined by their intra-retinal connections or by their intrinsic photosensitivity.

Chapter 3

Development of two types of murine melanopsin retinal ganglion cell

Abstract

Intrinsically photosensitive retinal ganglion cells (ipRGCs) contain the photopigment melanopsin and project to brain centers involved in entrainment of circadian rhythms and the pupillary light reflex. There are at least two ipRGC types in the mouse retina that relay illumination signals to the hypothalamic suprachiasmatic nucleus and olivary pretectal nucleus. A basic feature of the vertebrate visual system is the ON-OFF visual pathways that begin at the level of the retina. Prior to eye opening, conventional RGCs differentiate into ON or OFF types, which relies on signaling from rod and/or cone pathways. The goal of the present set of experiments was to use reporter mouse strains to test the hypothesis that ipRGCs develop in the same manner as conventional RGCs in the mouse retina. At birth, ipRGCs have not differentiated into two distinguishable cell types. By postnatal day 10, two distinct types of ipRGC could be identified, based upon the presence or absence of the reporter protein.ipRGC differentiation was delayed in mice dark reared from birth until after eye opening and in mice with pharmacological blockade of dopamine type 2 receptors. Taken together, the present results suggest that ipRGC development is similar to conventional RGC development in mouse retinas.

Introduction

A basic function of the vertebrate visual system is to detect light increments and decrements and to convey them to the brain through the ON-OFF parallel pathways. The retinal physiological (Hartline, 1938; Barlow, 1953), anatomical (Famiglietti and Kolb, 1979; Nelson et al, 1979) and molecular basis (Saito and Kaneko, 1983; Nawy and Jahr, 1990; Shiells and Falk, 1990) of ON-OFF parallel visual pathways have been extensively studied in the retina. Photoreceptors contact horizontal cells and bipolar cells in a single synaptic plexus known as the outer plexiform layer (OPL). The inner plexiform layer (IPL) is a synaptic lamina where bipolar and amacrine cell axon connections are made with retinal ganglion cell (RGC) dendrites within one of several synaptic layers. ON cell responding partners make synaptic connections confined to the inner (proximal to RGCs) region while OFF cells communicate within the outer (distal to RGCs) portion of the IPL (Famiglietti and Kolb, 1978; Nelson et al., 1979). These regions are termed the ON and OFF sublamina of the IPL, respectively.

Conventional mammalian RGCs are not differentiated into ON-OFF types at birth. This is exemplified by immature RGC dendrites ramifying diffusely throughout the entire extent of the IPL (Maslim and Stone, 1988; Tian and Copenhagen, 2003). RGC dendrites are 'pruned', or refined, throughout postnatal development. At eye opening, (e.g. mouse: ~ postnatal day [PD] 12) RGC dendrites are confined to either the ON or OFF sublamina of the IPL with a small subpopulation of RGCs sending dendrites into both the ON and OFF sublamina of the IPL (Maslim and Stone, 1988; Wong and Ghosh, 2002; Tian and

Copenhagen, 2003; Coombs et al., 2006). The precise mechanism of RGC dendrite refinement is currently under intense investigation (for review see Chalupa and Gunhurt, 2004; Tian, 2008).

Several key studies have implicated a role for the development of outer retinal neuronal pathways in RGC dendrite refinement. Conventional RGCs in animals deprived of cyclic light/ dark rearing (dark reared) from birth until after eye opening fail to show dendrite maturation in RGCs as noted by 'diffusely unstratified/ unramified' dendrites throughout the entire extent of the IPL. Accordingly, an unrefined/ immature RGC demonstrates physiological responses to light onset and offset (Tian and Copenhagen, 2003). Intraocular injection of the metabotropic glutamate receptor (mGluR6) agonist L-AP4, also known as APB, specifically hyperpolarizes ON bipolar cells. In the presence of L-AP4, ON bipolar cells are unresponsive to a light stimulus and consequently fail to signal postsynaptic RGCs. In cat, continuous intraocular administration of L-AP4 throughout retinal development retards RGC dendrite refinement (Bodnarenko et al., 1993) similar to dark reared animals reported by Tian and Copenhagen (2003). Taken together, these reports demonstrate that visual experience and more specifically neural transmission at the first retinal synapse (photoreceptor→ bipolar cell) is necessary for proper developmental maturation of RGC dendrite ramification in the IPL.

A nonconventional RGC type containing the photopigment melanopsin has recently been shown to be intrinsically photosensitive (ipRGCs)(Berson et al., 2002; Sekeran et al., 2003; Warren et al., 2003; Hartwick et al., 2007). ipRGCs

have been described in a variety of mammalian species including rat (Gooley et al., 2001; Hattar et al., 2002), mouse (Hattar et al., 2002; Provencio et al, 2002), hamster (Morin et al., 2003; Sollars et al., 2003), cat (Semo et al., 2005) non-human (Dacey et al., 2005) and human primates (Hannibal et al., 2004). ipRGCs relay illumination information to brain centers involved in the so called 'non-image forming' visual system including the suprachiasmatic nucleus (SCN) (Gooley et al., 2001; Hattar et al., 2002, 2006; Morin et al., 2003; Sollars et al., 2003; Baver et al., 2008), which is involved in circadian entrainment and the olivary pretectal nucleus (OPN) (Hattar et al., 2002, 2006; Gooley et al., 2003; Morin et al., 2003; Baver et al., 2008), that is involved in pupil constriction. While the developing retinal neural circuitry has been extensively examined for the classical image-forming visual system, the development of the retinal substrates involved in the non-image forming visual system remains poorly understood.

ipRGCs are photosensitive from birth, (Hannibal and Fahrenkrug, 2004; Sekaran et al., 2005) sending photic information to the SCN as early as PD 0 (Lupi et al., 2006). Interestingly, light input to the SCN is documented about 10 days prior to the development of rod and cone photoreceptor pathways (Ratto et al., 1991; Mumm et al., 2005) suggesting that rod and/or cone input is not necessary for sending photic cues to the SCN. At birth, the physiological responses of ipRGCs to light stimulation are much weaker, however, in comparison to firing characteristics in the adult retina (Tu et al., 2005; Schmidt et al., 2008). There are at least two ipRGC types in the adult mouse retina (Provencio et al., 2002 a, b; Tu et al., 2005; Baver et al., 2008; Schmidt and

Kofuji, 2009) called M1s and M2s. M1 ipRGC dendrites ramify closely to the inner nuclear layer (INL) in the OFF sublamina while the dendrites of M2s ramify in the ON sublamina of the IPL (Baver et al., 2008; Schmidt et al., 2008; Schmidt and Kofuji, 2009). Several studies have previously examined the development of ipRGC anatomy and physiology in animals lacking functional rod and cone photoreceptors (Fahrenkrug et al., 2004; Tu et al., 2005; Ruggiero et al., 2009). Direct synaptic input from the outer retina has been shown at the immunohistochemical, physiological and electron microscopic levels (Belenky et al., 2003; Dacey et al., 2005; Jusuf et al., 2007; Østergaard et al., 2007; Viney et al., 2007). To date, the role of rod and/or cone photoreceptor pathway development with regard to influencing ipRGC dendrite refinement and perhaps melanopsin expression remains unknown.

By targeting the *tau-lacZ* fusion gene to the melanopsin gene locus in mice, ipRGCs that would normally synthesize melanopsin express the marker enzyme β-galactosidase instead (Hattar et al., 2002, 2006). In the *tau-lacZ* $^{+/-}$ mouse, β-galactosidase-containing ipRGCs are a selective marker for M1 ipRGCs while β-galactosidase-lacking ipRGCs comprise M2s (Baver et al., 2008). The overall aim of the present study is to determine if ipRGCs develop in a manner similar to conventional ON and OFF RGCs. It is hypothesized that ipRGCs will be undifferentiated at birth and will diverge into distinct types prior to eye opening similar to conventional RGCs. A time course beginning at birth using the same criteria as described previously in Baver et al. (2008) is used to determine the developmental period of β-galactosidase-positive (BG+) or negative (BG-)

ipRGCs in *tau-lacZ*$^{+/-}$ mice. A second transgenic mouse line expressing green fluorescent protein (GFP) under the control of the melanopsin promoter (Schmidt et al., 2008) is also used to confirm previous criteria of BG+ and BG- discrimination observed in the *tau-lacZ* mouse (Baver et al., 2008).

A second set of experiments seeks to determine if visual experience is necessary for ipRGC refinement similar to conventional RGCs. If visual experience is necessary for ipRGC dendrite refinement it would be expected that rearing mice in different lighting regimes, such as dark rearing, would alter differentiation of ipRGCs.

Dopaminergic (DA) amacrine cells are presynaptic to ipRGCs (Østergaard et al., 2007; Vugler et al., 2007) and regulate expression of melanopsin mRNA (Sakamoto et al., 2005). The final experiment seeks to determine if DA transmission plays a role in melanopsin differentiation in development.

Materials and Methods

Animals

All experiments were performed according to the National Institutes of Health Guidelines for the Care and Use of Laboratory Animals and were approved by the Colorado State University Animal Care and Use Committee. Mice of a B6/129 strain in which *tau-lacZ* was targeted to the melanopsin gene locus were used in these studies; heterozygous tau-lacZ+/- mice produce both β-galactosidase and melanopsin. *Tau-lacZ*$^{+/-}$ knock-in mice raised in our laboratory were generously donated by Dr. Samer Hattar (Johns Hopkins

University). A second mouse strain (FVB/NCR) donated by Paulo Kofuji (University of Minnesota) in which the gene for the reporter green fluorescent protein (GFP) was driven by the mouse melanopsin promoter (Schmidt et al., 2008; Schmidt and Kofuji, 2009) was also used in the developmental time course study.

Animals were maintained under a 12 h light/12 h dark cycle with lights on (termed zeitgeber time [ZT] 0) at 0700 with food and water available *ad libitum*. Both male and female *tau-lacZ*$^{+/-}$ mice were sacrificed on postnatal day (PD) 0, 5, 7, 8,9,10 and adult (3-4 weeks of age) between 1100 and 1200 h (ZT 4-5)(N = 3/ time point). Both male and female mice in which GFP was driven by the mouse melanopsin promoter were sacrificed on PD 0,5,7,8,9,10,12,14 and adult (3-4 weeks of age) (N = 3/ time point). Male and female *tau-lacZ*$^{+/-}$ mice were born into constant dark (DD). Dark-reared mice were sacrificed after 21 days (N = 3).

Dopamine Pharmacology

Male and female *tau-lacZ*$^{+/-}$ mice were injected intraperitoneally (i.p.) every 12 hours (ZT 0 and 12) with the dopamine type 2 (D2) receptor antagonist (2 mg/kg) of (S)-(-) sulpiride (S7771-SG; Sigma Aldrich, St. Louis, MO) dissolved in 0.1% DMSO (N = 3) or equivalent volume of saline (N =3) from PD 2-17. Mice were maintained on a 12 h light/12 h dark schedule with lights on at 0700 and sacrificed between 1100 h and 1200 h (ZT 4 and ZT 5) on PD 17.

Immunohistochemistry

Animals were deeply anesthetized with sodium pentobarbital (80 mg/kg, i.p.) and perfused transcardially with 0.9% saline followed by cold freshly prepared fixative consisting of 4% paraformaldehyde in 0.1 M phosphate buffer (pH 7.3). Eyes were enucleated, anterior segments and vitreous were removed and eyecups were embedded in 7% gelatin (100 bloom, Fisher Scientific) and placed in the same fixative with 20% sucrose overnight at 4 °C. Eyecups were sectioned at 40 µm on a sliding microtome equipped with a freezing stage (Physitemp Instruments Inc., Clifton, NJ) and sections were collected in phosphate buffered saline (PBS).

The following antisera were used for immunohistochemistry: rabbit anti-melanopsin diluted 1:5000 (UF006 generously provided by Ignacio Provencio) and either chicken anti-β-galactosidase antibody diluted 1:500 for *tau-lacZ* mice (ab9361, Abcam, Cambridge, MA) or chicken anti-green fluorescent protein diluted 1:500 (GFP) (ab13970, Abcam) for mice containing the GFP reporter. Secondary antibodies used were produced in goat against the species for which the primary antiserum was generated (See below).

Light microscopic immunohistochemistry was performed on free-floating sections. The following procedure was performed at room temperature. After rinsing in PBS (pH 7.3), sections were transferred to a blocking solution in PBS containing 4% normal goat serum (NGS, Sigma), 0.4% triton X-100 (TX, Sigma) and 1% bovine serum albumin (BSA) and were then transferred to the primary antisera in PBS containing 1% NGS, 0.4% TX and1% BSA for 24 h. Primary

antisera were visualized with either a goat anti-rabbit IgG or goat anti-chicken IgY conjugated either to Alexa Fluor 488 or Alexa Fluor 594 (Molecular Probes) diluted 1:400 in PBS for 60 minutes. Sections were rinsed in PBS, mounted on subbed slides, coverslipped with Vectashield (Vector Laboratories, Burlingame, CA) and sealed with fingernail polish to prevent dehydration.

Data Analysis

Sections were analyzed on a Zeiss Axioplan 2 imaging epifluorescent microscope (Carl Zeiss Inc, Thornwood, NY) using optics for EGFP and Texas Red. Retinal sections were first examined for one label (e.g., Alexa Fluor 488) and then the other label (e.g., Alexa Fluor 594) with final confirmation of the analysis by examining both red and green signals concurrently using a dual band filter. The ratio of ipRGCs that are β-galactosidase-positive (BG+)/GFP+: β-galactosidase-negative (BG-)/GFP- were compared for each condition using analysis of variance followed by a Bonferroni contrast statistic with a p-value of 0.05 being accepted statistically significant. Student's t-test post-hoc analysis were used in *tau-lacZ*$^{+/-}$ mice that were included in DD reared and dopamine pharmacology studies with a p-value < 0.05 being accepted as statistically significant. All images were aquired on a Zeiss LSM 510 meta confocal microscope (Carl Zeiss Inc) with a 40X objective using LSM Image Browser software (Carl Zeiss Inc). Digital images were pseudo-colored in LSM Image Browser, and images were prepared using Adobe Photoshop version 6.0.1. Images were enhanced for brightness and/or contrast.

Results

Melanopsin expression throughout postnatal development

To determine if ipRGCs contained varying levels of melanopsin protein from birth we used two independent reporter mouse lines to label both M1s (BG+/GFP+) and M2s (BG-/GFP-) and examined ipRGCs at different postnatal times. Other laboratories (Hattar et al., 2006; Schmidt et al., 2008) have used M1 and M2 terminology to classify ipRGCs based strictly on where dendrites stratify in the IPL, therefore the BG+: BG-/GFP+:GFP- nomenclature shall be used throughout the remainder of the report.

Figure 3.1A shows both melanopsin (Figure 3.1A') and β-galactosidase-immunoreactive (Figure 3.1A") RGCs in a *tau-lacZ*$^{+/-}$ PD 0 mouse retina. At PD 0, mice in which the *tau-lacZ* fusion gene replaced one melanopsin gene almost all of the melanopsin ipRGCs were also immunoreactive for β-galactosidase. From a total of 2195 melanopsin positive cells, 2185 also express β-galactosidase (99.5 ± 0.2%; Table 3.1). Figure 3.1 B" shows β-galactosidase reactivity in both the ON and OFF sublamina of the IPL in a PD 7 *tau-lacZ*$^{+/-}$ mouse retina (arrows). Conversely, *tau-lacZ*$^{+/-}$ mice at PD 10 shows β-galactosidase immunoreactivity appearing to be restricted in the OFF-sublamina of the IPL (astericks) (Figure 3.1C"). Figure 3.2A shows both melanopsin (Figure 3.2A') and GFP-immunoreactive (Figure 3.2A") RGCs in PD5 mice in which the melanopsin promoter drives GFP. At PD 10, GFP (Figure 3.2B") is detected in some, but not all, melanopsin-immunoreactive ipRGCs (Figure 3.2B"'). Similar observations are made in adult mice in which GFP is driven by the

melanopsin promoter (Figure 3.2 C).

As shown in Tables 3.1 and 3.2, the ratio of BG+:BG-/GFP+:GFP- is similar in both reporter mouse strains throughout development. There is a significant difference ($p < 0.05$) in the ratio of BG+: BG- ipRGCs at PD 0 compared to adult (49.2 $\pm$ 3.2%) *tau-lacZ*$^{+/-}$ mice using Bonferonni's contrast stastic (Table 3.1). Similar results were observed between PD 0 (98.6 $\pm$ 0.4%) and adult (54.4 $\pm$ 2.6%) mice in which GFP was driven from the melanopsin promoter ($p < 0.0001$; Table 3.2). The ratio of BG+:BG- changes significantly between PD 9 (BG+: ~88%; BG-: ~12%) and PD 10 (BG+:~ 59%; ~BG-: 41%) ($p<0.05$, Bonferonni's contrast statistic)in *tau-lacZ*$^{+/-}$ mice (Table 3.1). Mice in which GFP was driven by the melanopsin promoter yielded similar results compared to *tau-lacZ*$^{+/-}$ mice. The ratio of GFP+:GFP- changes significantly between PD 9 (GFP+: ~85%; GFP-:~15%) and PD 10 (GFP+: ~57%; GFP-: ~43%) ($p<0.05$, Bonferonni's contrast statistic) (Table 3.2).

	PD 0	PD5	PD 7	PD 8	PD 9	PD 10	Adult
Mel + β-gal/	2185/	1459/	679/	1049/	969/	786/	454/
Mel	2195	1489	715	1079	1110	1331	923
Percent	99.5	97.9	95.0	97.2	87.3	59.1	49.2

Table 3.1. The ratio of BG+:BG- changes from birth to adulthood in *tau-lacZ*$^{+/-}$ mice. Retinal sections from both eyes of *tau-lacZ*$^{+/-}$ mice were double labeled for β-galactosidase (β -gal) and melanopsin (Mel) antibodies. Almost all RGCs identified with the melanopsin antibody also express β-gal at PD0, PD5, PD7, PD8, PD9 whereas about half of ipRGCs contain β-gal at PD10 and adulthood.

	PD 0	PD5	PD 7	PD 8	PD 9	PD 10	PD 12	PD14	Adult
Mel +GFP/	1057/	231/	2864/	292/	532/	680/	744/	118/	970/
Mel	1075	233	3106	326	627	1195	1227	227	1757
Percent	98.3	99.1	92.2	89.6	84.8	56.9	60.6	52.0	54.1

Table 3.2. The ratio of GFP+:GFP- changes from birth to adulthood in melanopsin-GFP mice. Retinal sections from both eyes of GFP-heterozygous mice were double labeled for green fluorescent protein (GFP) and melanopsin (Mel) antibodies. Almost all RGCs identified with the melanopsin antibody also express GFP at PD0, PD5, PD7, PD8, PD9 whereas about half of ipRGCs contain GFP at PD10, PD12, 14 and adulthood.

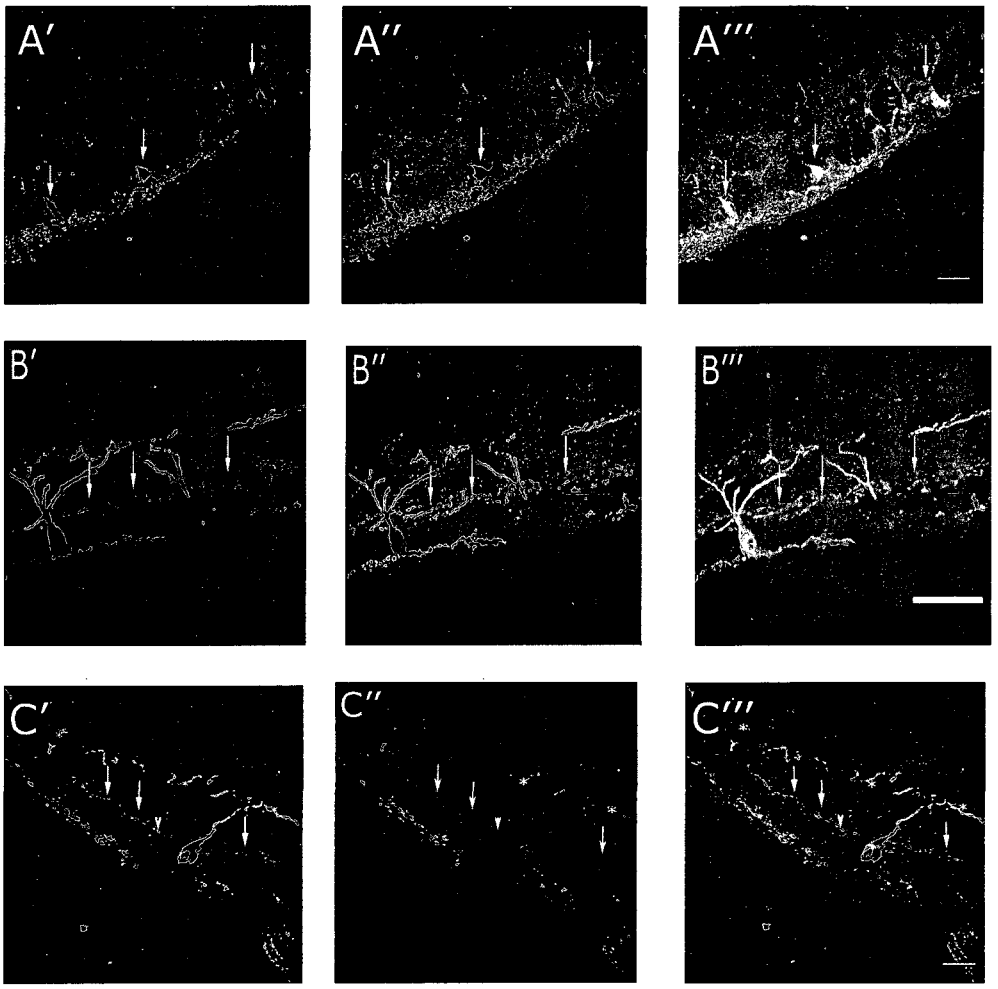

Figure 3.1. The ratio of BG+:BG- ipRGCs changes in postnatal development. A) ipRGCs in PD 0 *tau-lacZ*$^{+/-}$ retinal sections double labeled with an antiserum directed against the amino-terminus of the mouse melanopsin protein (A') and β-galactosidase (A''). A''' is merged of A' and A''. Arrows indicate typical cells that were used to quantify double labeling of melanopsin and β-galactosidase. Scale bar: 20 μm B) ipRGCs in PD 7 *tau-lacZ*$^{+/-}$ retinal sections double labeled with an antiserum directed against the amino-terminus of the mouse melanopsin protein (B') and β-galactosidase (B''). B''' is merged of B' and B''. Scale bar: 50 μm. Arrows in B'' indicate labeling of the ON sublamina of the IPL in PD 7 mouse retina. C) ipRGCs in PD 10 *tau-lacZ*$^{+/-}$ retinal sections double labeled with an antiserum directed against the amino-terminus of the mouse melanopsin protein (C') and β-galactosidase (C''). C''' is merged of C' and C''. Asterick indicates labeling of the OFF sublamina using both melanopsin (C') and β-galactosidase (C'') antisera. Arrows in C' indicate labeling of the ON sublamina of the IPL in PD 7 mouse retina which is absent in C". Arrowhead indicates a BG- ipRGC.

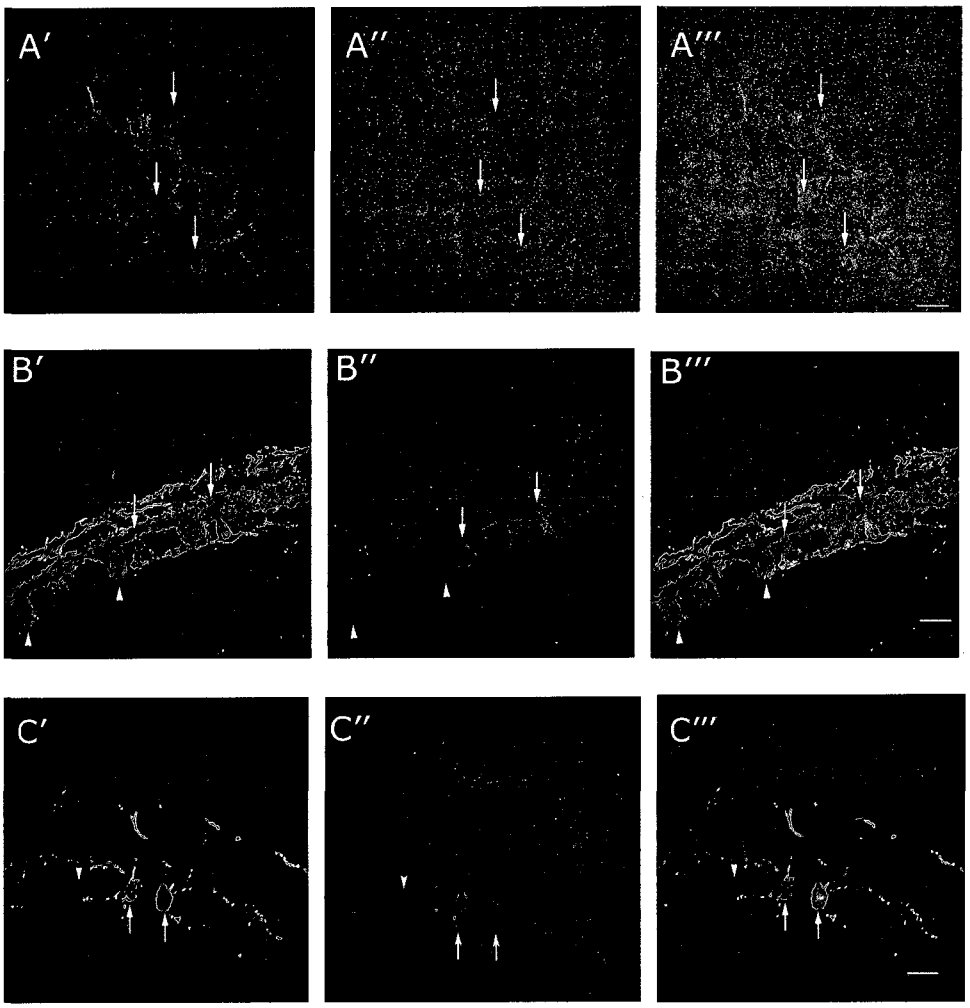

Figure 3.2. The ratio of GFP+:GFP- ipRGCs changes in postnatal development. A) ipRGCs in PD 5 melanopsin-GFP heterozygous retinal sections double labeled with an antiserum directed against the amino-terminus of the mouse melanopsin protein (A') and GFP (A"). A"' is merged of A' and A". Arrows indicate typical cells that were used to quantify double labeling of melanopsin and GFP. Scale bar: 20 μm B) ipRGCs in PD 10 melanopsin-GFP heterozygous retinal retinal sections double labeled with an antiserum directed against the amino-terminus of the mouse melanopsin protein (B') and GFP (B"). B"' is merged of B' and B". Arrows indicate labeling of GFP+ ipRGCs while arrowheads indicate GFP- ipRGCs. C) ipRGCs in adult (3-4 weeks) melanopsin-GFP heterozygous retinal retinal sections double labeled with an antiserum directed against the amino-terminus of the mouse melanopsin protein (C') and GFP (C"). C"' is merged of C' and C". Arrows indicate labeling of GFP+ ipRGCs while arrowhead indicates a GFP- ipRGC.

Constant Dark Rearing

Dark rearing mice from birth until PD 21 retards segregation of RGCs from ON-OFF to ON and OFF morphological types (Tian and Copenhagen, 2003; Tian, 2008). To determine whether DD alters the development of ipRGCs, *tau-lacZ*$^{+/-}$ mice were dark reared for 21 days. Figure 3.3 shows an ipRGC that appears to send dendrites that stratify only in the ON sublamina of the IPL stained with a melanopsin antiserum directed against the amino-terminus of the mouse melanopsin protein (A) and β-galactosidase (B). From the 1552 ipRGCs labeled, 1294 cells were also β-galactosidase-immunoreactive (83.4%, N = 3). There is a significant difference in the BG+:BG- ratio when comparing DD PD 21 (N = 3) and adult *tau-lacZ*$^{+/-}$ mouse retinas using a student's t-test ($p < 0.0006$). Thus, it appears that the absense of light results in a retardation of BG+:BG- differentiation in the *tau-lacZ*$^{+/-}$ mouse.

Figure 3.3. A greater proportion of ipRGCs are BG+ in DD reared animals compared to animal raised in 12 h light/12 h dark cycle. ipRGCs in dark reared PD 17 *tau-lacZ*$^{+/-}$ retinal sections double labeled with an antiserum directed against the amino-terminus of the mouse melanopsin protein (A) and β-galactosidase (B). C is merged A and B. Arrows indicate labeling of an M2 ipRGC type that appears to ramify in the ON sublamina of the IPL. Scale bar: 20 μm.

Dopamine Pharmacology

To determine whether dopamine plays a role in the development of ipRGCs *tau-lacZ*$^{+/-}$ mouse pups were injected every 12 hours (ZT 0 and ZT 12) beginning at PD 2 with the D2 receptor antagonist sulpiride (2.0 mg/kg; i.p.) or with a comparable volume of saline for control mice. Animals were sacrificed at PD 17 at ZT 4. In control mice (N = 3), 340 of the 621 ipRGCs also contain β-galactosidase (54.8%; Figure 3.4). From the 1380 melanopsin-immunopositive ipRGCs labeled, 1183 cells colabeled with β-galactosidase (Figure 3.4). There was a significant increase in *tau-lacZ*$^{+/-}$ mice in the proportion of ipRGCs labeled with the melanopsin antiserum that contained β-galactosidase in the sulpiride treated (BG+: 83.3%) than control (BG+: 54.8%) ($p < 0.0003$) using a Student's t-test.

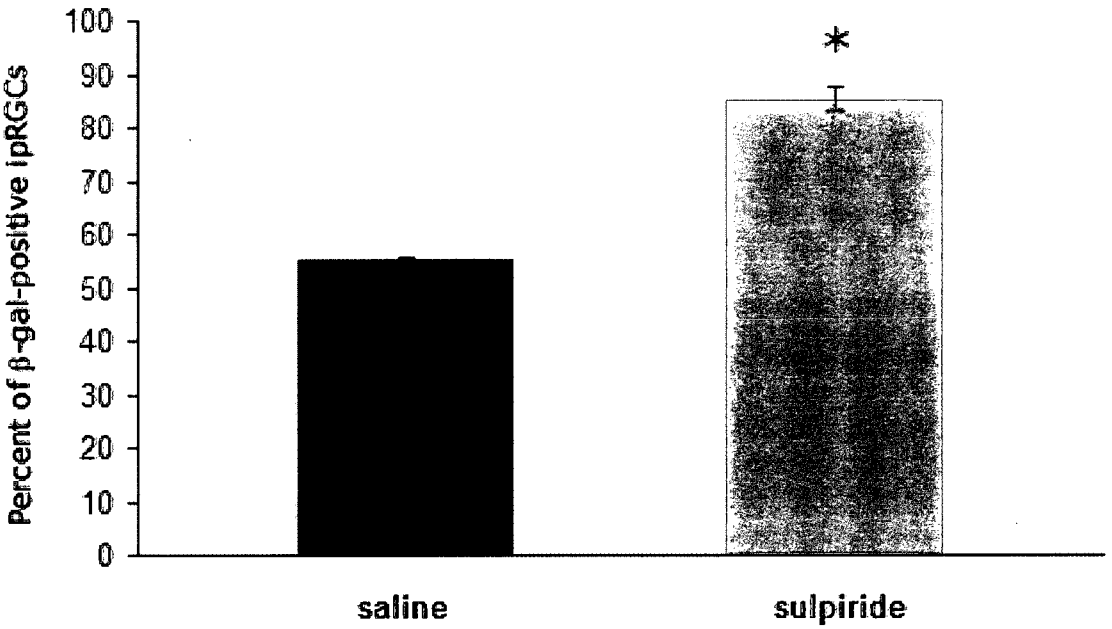

Figure 3.4. (Previous page) Addition of dopamine antagonist decreases the proportion of BG+ ipRGCs. The ratio of BG+:BG- is higher in *tau-lacZ*$^{+/-}$ mice chronically injected (i.p.) with the dopamine type 2 receptor (D2) antagonist sulpiride (2 mg/ kg) from PD 2 to PD 17 compared to saline injected controls. *p< 0.01.

Discussion

The suprachiasmatic nucleus is light responsive by PD 0 which has been demonstrated by the induction of the immediate early gene protein product c-Fos (Lupi et al., 2006). ipRGCs are intrinsically photosensitive at birth (Hannibal and Fahrenkrug, 2004). Rod and cone photoreceptor pathway synaptogensis is completed by ~PD10, indicating that classical photoreceptors are not necessary for signaling photic cues for synchronizing circadian rhythms. The primary finding in the present study is that the amount of reporter protein observed in ipRGCs changes so that by P10 the profile approximates that of the adult retina (Figure 3.1, Tables 3.1 and 3.2). These results were obtained in experiments using two independent types of mouse lines in which the melanopsin protein was replaced by either the *tau-lacZ* fusion protein or green fluorescent protein. While rod and/or cone photoreceptors are not essential to convey light cues to the suprachiasmatic nucleus prior to eye opening, it is possible that classical photoreceptor pathways play a role in RGC dendrite refinement.

There are three distinct phases in retinal synaptic development, with the lateral pathways (amacrine and horizontal cells) developing prior to vertical pathways (cone photoreceptors → bipolar cells → RGCs) proposed originally by Fisher (1979). First, amacrine cell processes form synaptic contacts with RGC dendrites in the inner retina. This is followed by outer retinal synaptogenesis, as

exemplified by contacts between rod and cone photoreceptors and horizontal cells. Bipolar cell synapse formation on both photoreceptors and RGC dendrites is the final phase in synaptic development, which allows for a functional retinal circuit. The final phase of synaptic development in mouse retina occurs at about ~PD 10 with the development of bipolar cell synapses and thus functional rod/cone photoreceptor pathways (Fisher et al, 1979). This is the same time period that distinct ipRGC types develop. Thus, bipolar cell synaptogensis may be important for ipRGC dendrite refinement. The identity of presynaptic retinal neurons to ipRGCs, however, is not completely understood.

In the vertebrate retina, RGCs respond to light increments (ON responding), light decrements (OFF responding) or transiently to light increments and light decrements (ON-OFF responding) (Chalupa and Gunham, 2004). Melanopsin RGCs are intrinsically photosensitive yet are synaptically driven by rod and/or cone photoreceptor pathways in response to light increments (Dacey et al., 2005; Wong et al., 2007; Pickard et al., 2009).

The alpha and beta classes of conventional RGC are comprised of anatomically distinct cell types based on dendrite ramification in the IPL corresponding to physiological ON and OFF responses to a light stimulus (Boycott and Wässle, 1974; Fukada et al., 1985). Anatomically, ipRGCs can be subdivided into distinct types based on where dendrites ramify in the IPL. M1 ipRGCs ramify in the OFF sublamina, M2 ipRGCs ramify in the ON sublamina of the IPL and a third type of ipRGC ramifies both the ON and OFF sublamina of the IPL (Provencio et al., 2002b; Baver et al., 2008; Schmidt and Kofuji, 2009). ON/OFF

segregation of ipRGCs can be observed at ~ PD 6 (Tu et al., 2005), revealed by immunohistochemistry using an amino-terminus antiserum directed against the mouse melanopsin protein (Provencio et al., 2002a). In adult *tau lacZ*$^{+/-}$ mice, β–galactosidase-positive ipRGCs contain dendrites stratifying in only the OFF sublamina of the IPL (Hattar et al., 2002, 2006; Baver et al., 2008; Pickard et al., 2009). Use of a commercially available antiserum directed against β-galactosidase produces results that suggest that ipRGCs ramify in both the ON and OFF sublamina of the IPL at PD 7 (Figure 3.2B"). It is not until ~ PD 10 that the distinction of two cell types of ipRGC emerges and β-galactosidase immunoreactivity is restricted to the OFF sublamina of the IPL. It is important to note that the ipRGC dendrites may not be unstratified/ multistratified as reported in conventional RGCs (Bodanerko et al., 1993; Tian and Copenhagen, 2003). Sekeran et al. (2005) reported that at PD 5 the number of β-galactosidase-positive ipRGCs is five times greater than that of the adult retina. The authors suggest this decline is due to developmental apoptosis (Sekeran et al, 2005). Alternatively, levels of β-galactosidase may become undetectable throughout the development of outer retinal synapses in a population of ipRGCs.

In adult retinas, ON and OFF RGCs are differentially innervated by bipolar and amacrine cells in the IPL. Light refines dendrite ramification in the IPL into ON or OFF RGCs, throughout development (Tian and Copenhagen, 2003, Tian, 2008). Persistent intraocular administration of the mGluR6 agonist L-AP4, which inactivates the ON pathway, results in a retardation of ON/OFF segregation (Bodanerko et al., 1993). Furthermore, mice reared in constant darkness into

adulthood fail to show RGCs with refined dendrites (Tian and Copenhagen, 2003). Taken together, these results suggest that rod and cone photoreceptor pathway activity is necessary for proper ON-OFF RGC pathway segregation. Consistent with conventional RGCs, ipRGC developmental differentiation into types discernible on the basis of protein expression is inhibited in mice reared in constant darkness (Figure 3.3). It appears that ipRGC cell type differentiation is also dependent on signaling from the outer retina. One experiment to confirm the role of photoreceptor activation on ipRGC refinement would be to use a mouse in which rod and cone photoreceptors are not functional crossed with the *tau-lacZ* reporter mouse. The guanylate cyclase double knock out mouse generated by Baehr and colleagues (2007) could be optimal for determining the importance of photoreceptors on ipRGC developmental refinement. This is an optimal model because photoreceptors are non-functional from birth. However, ipRGCs have been shown to be presynaptic to dopaminergic (DA) amacrine cells (Zhang et al, 2008), which in turn synapse on ipRGCs (Østergaard et al., 2007; Vugler et al., 2007). It is therefore possible that ipRGCs regulate the development of where dendrites ramify in the IPL. Thus, in photoreceptor dysfunctional mice, it is possible that there is an alternative developmental mechanism through this ipRGC → DA amacrine cell → ipRGC pathway resulting in cell type segregation.

As noted previously, DA amacrine cells are presynaptic to ipRGCs (Østergaard et al., 2007; Vugler et al., 2007) and have been implicated in regulating melanopsin expression in ipRGCs (Sakamoto et al., 2005). Using *in situ* hybridization, D2 receptors have been localized on ipRGCs (Sakamoto et al.,

2005). We sought to determine the role of DA transmission on the development of ipRGCs by pharmacologically inhibiting D2 receptors in mouse pups. Another important finding in this study is that DA transmission is important for ipRGC development. Specifically, injection of the D2 receptor antagonist sulpiride (2 mg/kg) in mice PD 2- PD 17 results in the retardation of BG+:BG- differentiation. One interpretation of these results is that the D2 blockade retards the developmental down regulation of β-galactosidase expression and thus the percentage of double-labeled cells remains high. An alternative interpretation is that inhibition of DA transmission on D2 receptors located on ipRGCs results in a direct retardation of dendrite refinement. It is also important to point out that mice were injected with sulpiride dissolved in DMSO or saline. It is unkown whether DMSO affects the ratio of β-galactosidase in ipRGCs.

D2 receptors are also localized on different retinal cell populations including photoreceptors and DA amacrine cells (Ngyun-Legros et al., 1999). DA amacrine cells send a considerable number of inputs to AII amacrine cells (Voigt and Wässle 1987; Kolb et al., 1991). AII amacrine cells are primarily driven by rod photoreceptor activation (Bloomfield et al., 1992; Dacheux and Raviola, 1986; Nelson, 1982). Perhaps, inhibiting dopamine transmission affects ipRGC differentiation through AII amacrine cells. D2 receptors are also autoreceptors on DA amacrine cells; activation of the D2 receptor on DA amacrine cells inhibits the firing and consequently results in a decrease of neurotransmitter (GABA and dopamine) release. It is plausible that normal DA transmission is essential for ipRGC dendrite refinement, either directly or indirectly via rod/ cone pathway(s).

In summary, ipRGCs are not fully differentiated at birth and become segregated into BG+ and BG- cell types at PD 10. As with conventional RGCs, ipRGC differentiation is dependent on visual experience, thus, classical rod and cone photoreceptor activation may also be necessary for ipRGC dendrite refinement. DA transmission acting via D2 receptors is also needed throughout development for BG+ and BG- ipRGC differentiation. BG+ and BG- ipRGCs probably contain differing levels of melanopsin protein content. Although classical rod and cone photoreceptor pathways synaptically drive depolarizations in ipRGCs, a further role of classical photoreceptor pathways may be to regulate the expression of melanopsin protein in ipRGCs.

Chapter 4

General Discussion

The recently discovered melanopsin-expressing intrinsically photosensitive retinal ganglion cell (ipRGC) has complicated the conventional examination of retinal cellular anatomy, circuitry and physiology. Conventional RGCs receive input from bipolar cells either responding to light increments, light decrements or both. The synapses of ON and OFF bipolar cells onto respective RGCs are located in a predictable portion of the inner plexiform layer (IPL) (Famiglietti and Kolb, 1976). Thus, RGCs that respond to light increments will have dendrites that ramify closer to the ganglion cell layer while RGCs responding to light decrements possess dendrites that ramify closer to the inner nuclear layer (INL).

Melanopsin RGCs are certainly not conventional RGCs considering the intrinsic response to light stimulation in the total absence of rod/cone input (Berson et al., 2002; Warren et al., 2003; Hartwick et al., 2007). Conventional RGC types also tile the retina in a 'non-random' array (Peichl and Wässle, 1981; Wässle et al, 1981a, b), which is another contrasting feature of ipRGCs compared to conventional RGCs (Semo et al., 2005). Specifically, Semo et al. (2005) have shown that ipRGCs are randomly distributed in the cat retina.

Determining how to differentiate two types of ipRGC in the mouse retina

Dendrites of ipRGCs have added further complexity that must be established to grasp a full understanding of the underlying outer retinal circuitry involved in signaling ipRGCs. The length of ipRGC dendrites is ~150 μm in rat (Hattar et al., 2002) and gerbil (Fite et al., 2003), which is greater than most conventional RGC dendrites (Coombs et al., 2006). Using an antiserum directed against the mouse melanopsin protein, two populations of ipRGC were originally identified in mouse retinas (Provencio et al., 2002a,b). These two populations were originally delineated based on variation of staining intensity following immunohistochemical procedures (Provencio et al., 2002b) and were classified as M1s (darkly stained) or M2s (lightly stained). More conventional anaylsis showed that M1s and M2s also differ in the total number of primary dendrites and soma size (Provencio et al., 2002b). However, the 'meshwork' of melanopsin dendrites first reported by Provencio and coworkers (2002a) together with the long length of dendrites made it difficult to quantify dendrite ramification as being strictly ON, OFF or ON-OFF ipRGC types.

To circumvent discriminating ipRGC types by the parameters used for classical RGCs, Chapter 1 utilzed the *tau-lacZ* knock-in mouse to differentiate between M1 and M2 ipRGCs Baver et al. (2008). It was shown that β-galactosidase, which is the protein product of the *tau-lacZ* gene, positively identifies only one-half of the ipRGCs labeled when using the amino-terminal mouse melanopsin antiserum (Provencio et al., 2002a). This population of ipRGCs is termed M1s, while β-galactosidase-negative ipRGCs are termed M2s.

Furthermore, M1 ipRGC dendrites ramify in the OFF sublamina of the IPL while M2 ipRGC dendrites appeared to ramify in the ON sublamina of the IPL. These observations were confirmed by Kofuji and colleagues (Schmidt et al., 2008; Schmidt and Kofuji, 2009) using a mouse in which green fluorescent protein (GFP) was being driven by the melanopsin promoter. By intracellular injection of ipRGCs with Lucifer yellow, Schmidt et al. (2008) and Schmidt and Kofuji (2009) showed that M1 ipRGC dendrites do in fact ramify in the OFF sublamina while M2 dendrites ramify in the ON sublamina of the IPL.

In mouse, M1s were also labeled specifically with an antiserum directed at the carboxyl-terminus of the rat melanopsin protein. Labeling one population of ipRGCs makes it possible to study the melanopsin system in the wild-type mouse retina. This negates the need for transgenic mouse breeding for experiments such that look at the variation of ipRGCs throughout the light/ dark cycle or dendrite ramification of M1s after prolonged exposure to DD (not shown). To date, there is no known antiserum that selectively identifies the M2 subpopulation. Recently, Ingham et al. (2009) used a toxin, saporin, conjugated to an extracellular melanopsin antibody to selectively ablates ipRGCs in rat. The authors propose that the rat retina contains two types of ipRGC similar to mouse and that saporin conjugated to melanopsin ablates the M1 population of ipRGCs. If M2 ipRGCs do survive then injection of the toxin followed by immunohistochemistry using the amino-terminus mouse melanopsin antisera would allow for visualization of only M2s. Morin and colleagues (Göz et al., 2008) have a saporin conjugated melanopsin antibody that ablates ~57.0% of ipRGCs. It is possible that these

remaining cells are M2 ipRGCs and studies similar to those mentioned above could be carried out to determine the fate of M2s (BG-) in 12 h light/12 h dark cycle.

The *tau-lacZ* knock-in mouse was generated to determine the central projections of ipRGCs (Hattar et al., 2006). However, this mouse contains only half (M1s) of the total extent of ipRGC projections. We have demonstrated that almost all (~98%) of the RGCs projecting to the suprachiasmatic nucleus (SCN), along the retinohypothamic tract, are melanopsin-expressing ipRGCs. Approximately 80% of the SCN projecting cells are M1s while the remaining 20% are M2s. Original reports suggested that ipRGCs projected to the outer 'shell' of the olivary pretectal nucleus (OPN) (Hattar et al., 2002, 2006; Gooley et al., 2003). We find that M1s predominantly project to the outer shell as originally suggested while M2s possibly project to the inner core (data not shown) (Baver et al., 2008). The remaining central projections of M2s are currently unknown; however, Hattar and colleagues (2009) have generated a transgenic mouse containing an axonal marker for both M1s and M2s similar to the *tau-lacZ* mouse. The authors show that M2s project to the lateral geniculate complex, which is involved in image-formation, suggesting that ipRGCs may be important for both non-image and image forming visual behaviors (Hattar et al., 2009).

The development of two types of ipRGC happens at a critical period in the mouse retina

The SCN receives light input at PD 0, which is most likely from ipRGC signaling because classical photoreceptors and pathways are not fully functional until ~PD 10 (Ratto et al., 1991, Mumm et al., 2005). Behavioral running wheel and pupil constriction data in adult mice lacking functional rod and cone photoreceptors also suggest that classical photoreception is not necessary for light cues being relayed to either the SCN or OPN (Lucas et al., 2001). The role of rod/cone photoreceptors with regard to the melanopsin system may be to regulate the level of protein, which may ultimately regulate firing characteristics of ipRGCs. Using the *tau-lacZ* knock-in (Hattar et al., 2002; 2006) and a mouse in which GFP is being driven by *Opn4* (Schmidt et al., 2008; Schmidt and Kofuji, 2009) mouse models, Chapters 3 and 4 (see below) begin to elucidate the role for rod and/or cone photoreceptor pathways regulating melanopsin expression in ipRGCs.

The retina has three distinct phases of synaptogensis according to Fisher (1979). First, amacrine cell processes form synaptic contacts with RGC dendrites in the inner retina ~PD 5. This is followed by outer retinal synaptogenesis (i.e. rod and cone photoreceptors and horizontal cell contacts). Bipolar synapse formation on both photoreceptors and RGC dendrites is the final phase in synaptic development. After bipolar cell synapses are formed, there is a functional retinal circuit from photoreceptors→ RGCs→ visual centers in the brain. The final phase of synaptic development in mouse retina occurs at about ~PD 10 with the development of bipolar cell synapses and thus functional rod/ cone photoreceptor

pathways (Fisher et al., 1979). Using previously described terminology (Baver et al., 2008), ipRGC differentiation occurs at PD 10 in two independent transgenic mouse lines, which coincidentally is at the same time that rod/cone transmission to RGCs becomes functional (Ratto et al., 1991, Mumm et al., 2005). Interestingly, ipRGC cell responses change in intensity at ~ PD 10 (Tu et al., 2005). Using a multielectrode array to record light responses from ipRGCs, Tu et al. (2005) demonstrated that at birth to ~PD 8 ipRGC responses were weak, while at PD 10 responses were more intense. Perhaps rod/cone photoreceptors drive melanopsin expression to higher levels for a greater light response. Another possibility is that rod/cone photoreceptor pathways directly depolarize ipRGCs as suggested in primate (Dacey et al., 2005) rat (Wong et al., 2007) and mouse (Pickard et al., 2009). Nevertheless, rod and cone photoreceptor pathways appear to regulate the firing characteristics in ipRGCs by mechanisms that are not completely understood.

Conventional RGC development relies on glutamatergic drive from the outer retina (Gunham and Chalupa, 2004). Tian and Copenhagen (2003) elegantly demonstrated that ON and OFF segregation is delayed in mice reared in constant darkness. ipRGC differentiation also appears to be delayed in mice reared in darkness from birth until three weeks of age. Specifically, data presented in Chapter 3 demonstrates the retardation of BG+:BG-refinement in animals reared in constant darkness for ~3 weeks. Furthermore, dopaminergic (DA) transmission also plays a role in the development of ipRGC cell type differentiation in *tau-lacZ* mice. Although conventional RGCs rely on cues from

rod/cone photoreceptor pathways, the dependence of ipRGC differentiation on conventional photoreceptor pathways or a possible role of melanopsin phototransduction in ipRGC differentiation remains unknown.

Melanopsin expression in ipRGCs of adult mice

It appears that rod/cone photoreceptors contribute to ipRGC refinement and possibly melanopsin expression regulation. The role of rod and cone photoreceptors on melanopsin expression regulation in adult animals remains poorly understood. Classically, rod and cone photoreceptors signal bipolar cells which signal amacrine and RGCs. Conventional RGCs integrate synaptic input from bipolar and amacrine cells which results in depolarization or hyperpolarization. ipRGCs also receive input from the outer retina (Belenky et al., 2003; Jusuf et al., 2007; Østergaard et al., 2007; Viney et al., 2007). Independent of melanopsin phototransduction, rod and/or cone photoreceptors synaptically depolarize ipRGCs (Dacey et al., 2005; Wong et al., 2007; Pickard et al., 2009). Presumably, rod and cone photoreception acts to modify the membrane potential of ipRGCs, thus increasing or decreasing the threshold for firing following light stimulation. GABAergic input comprises about half of the presynaptic input to ipRGCs (Belenky and Pickard, 2003); rod/cone signaling could therefore be capable of modifying the intrinsic light response in ipRGCs.

Recent evidence has suggested rod and cone photoreceptor pathways may also be involved in regulating melanopsin expression. Melanopsin mRNA decreases corresponding to photoreceptor degeneration, in the Royal College of

Surgeons (RCS) rat (Sakamoto et al., 2004). Vugler et al. (2008) noted a decrease in total number of ipRGCs in the RCS rat. Acute photoreceptor degeneration using the toxin N-methyl-N-nitrosourea (MNU) results in decreased melanopsin mRNA and apparent decrease of melanopsin immunoreactivity in dendrites of ipRGCs (Wan et al., 2006). These results were obtained in rat and challenge evidence originally established in mouse by Foster and colleagues (Semo et al., 2003). Original reports suggest that the level of melanopsin mRNA in a mouse model in which rods and cones were ablated (retinal degenerate coneless; *rd/rd, cl*) was indistinguishable from littermate controls. Conversely, mice lacking RPE65, a protein that is required for regeneration of visual chromophore in rods and cones show severe melanopsin protein immunoreactivity reduction. Melanopsin immunoreactivity is restored in RPE65 knockout mice carrying a transgene that selectively ablates rod photoreceptors (Doyle et al., 2006). It is therefore possible that retinal remodeling upon rod photoreceptor degeneration results in the appearance of normal ipRGC anatomy. Alternatively, photoreceptor degeneration in *rd/rd; cl* mouse retinas might not begin until adulthood (Carter-Dawson et al., 1978), which is when Semo et al. (2003) examined the mice. Taken together, this may explain the discrepancy between results in the RCS rat and the *rd/rd;* cl mouse. One possibility that warrants examination is that the relative levels of melanopsin expression in the retinal degenerate mouse model throughout photoreceptor loss similar to experimental procedures reported in rat.

In summary, this thesis has developed a mouse model to differentiate two populations of ipRGC and further show these cells have different central projections in non-image forming visual targets. These two cell types also ramify in different regions of the inner plexiform layer; the expression of melanopsin appears to correlate with the location of dendrite ramification in the IPL. Differential melanopsin expression is not apparent in developing ipRGCs until PD 10 and appears to be dependent on rod/cone photoreception. In adult retinas, melanopsin expression varies throughout the light/ dark cycle. Rod and cone photoreceptor pathways contribute to melanopsin variation in ipRGCs. The intricate retinal circuitry involved in ipRGCs may allow for non-image forming brain regions such as the SCN and OPN to be able to integrate illumination.

References

Avivi A, Oster H, Joel A, Beiles A, Albrecht A, Nevo E. 2004. Circadian genes in a blind subterranean mammal III: molecular cloning and circadian regulation of cryptochrome genes in the blind subterranean mole rat, *Spalax ehrenbergi* superspecies. J Biol Rhythms 19:22-34.

Baehr W, Karan S, Maeda T, Luo DG, Li S, Bronson JD, Watt CB, Yau KW, Frederick JM, Palczeksi K. 2007. The function of guanylate cyclase 1 and guanylate cyclase 2 in rod and cone photoreceptors. J Biol Chem. 282: 8837-8847.

Barnard AR, Appleford JM, Sekaran S, Chinthapalli K, Jenkins A, Seeliger M, Biel M, Humphries P, Douglas RH, Wenzel A, Foster RG, Hankins MW, Lucas RJ. 2004. Residual photosensitivity in mice lacking both rod opsin and cone photoreceptor cyclic nucleotide gated channel 3 alpha subunit. Vis Neurosci 21:675-83.

Barlow, HB. 1953. Summation and inhibition in the frog's retina. J. Physiol. Lond. 137: 327-337.

Baver SB, Ritchie S, Bittman EL, Fite KV. 2004. Melanopsin-immunoreactive retinal ganglion cells in the mouse retina. SfN abstract.

Baver SB, Pickard GE, Sollars PJ, Pickard GE. 2008. Two types of melanopsin retinal ganglion cell differentially innervate the hypothalamic suprachiasmatic nucleus and the olivary pretectal nucleus. Eur J Neurosci 27:1763-70.

Belenky MA, Smeraski CA, Provencio I, Sollars PJ, Pickard GE. 2003. Melanopsin retinal ganglion cells receive bipolar and amacrine cell synapses. J Comp Neurol 460: 380-393.

Belenky MA, Pickard GE. 2003. Melanopsin retinal ganglion cells Receive GABAergic input. Soc Neurosci Abs 513.2.

Bellingham J, Wells DJ, Foster RG. 2003. In silico characterization and chromosomal localization of human RRH (periopsin)- implications for an opsin evolution. BMC Gen 4:3.

Bergstrom AL., Hannibal J., Hinderson P., Fahrenkrug J. 2003. Light induced phase shift in the Syrian hamster (Mesocricesus auratus) is attenuated by the PACAP receptor antagonist PACAP6-38 or PACAP immunoneutralization. Eur J Neurosci 18:2552-2562.

Berson DM., Dunn FA., Takao M. 2002. Phototransduction by retinal ganglion cells that set the circadian clock. Science 295:1070-1073.

Berson DM. 2003. Strange vision: ganglion cells as circadian photoreceptors. Trends Neurosci 26:314-320.

Bishop PO. 1984. Processing of visual information within the retinostriate system. In: *Handbook of Physiology* (I. Darien-Smith, ed.). 341-424.

Bloomfield SA, Dacheux RF. 2001. Rod vision: pathways and processing in the mammalian retina. Prog Retin Eye Res. 20:351-384.

Bodnarenko SR, Chalupa LM. 1993. Stratification of ON and OFF ganglion cell dendrites depends on glutamate-mediated afferent activity in the developing retina. Nature.;364: 144-146.

Boldogkoi Z, Balint K, Awatramani GB, Balya D, Busskamp V, Viney TJ, Lagali PS, Duebel J, Pásti E, Tombácz D, Tóth JS, Takács IF, Scherf BG, Roska B. 2009. Genetically timed, activity-sensor and rainbow transsynaptic viral tools. Nat Methods. 6:127-130.

Boycott BB, Wässle H. 1974. The morphological types of ganglion cells of the domestic cat's retina. J Physiol. 240:397-419.

Boycott B, Wässle H. 1999. Parallel processing in the mammalian retina: the Proctor Lecture. Invest Ophthalmol Vis Sci. 40:1313-1327.

Carter-Dawson LD, LaVail MM, Sidman RL. 1978. Differential effect of the rd mutation on rods and cones in the mouse retina. Invest Opthalmol Vis Sci. 17:489-498.

Chalupa LM, Günhan E. 2004. Development of On and Off retinal pathways and retinogeniculate projections. Prog Retin Eye Res. 23:31-51.

Clarke, RJ, Ikeda H. 1985. Luminance and darkness detectors in the olivary and posterior pretectal nuclei and their relationship to the pupillary light reflex in the rat. I. Studies with steady luminance levels. Exp. Brain. Res., 57, 224-32.

Chávez AE, Singer JH, Diamond JS. 2006. Fast neurotransmitter release triggered by Ca influx through AMPA-type glutamate receptors. Nature. 443:705-708.

Coombs J, van der List D, Wang GY, Chalupa LM. 2006. Morphological properties of mouse retinal ganglion cells. Neuroscience. 140:123-136.

Costa MSMO, Santee UR, Cavalcante JS, Moraes PRA, Santos NP, Britto LRG. 1999. Retinohypothalamic projections in the common Marmoset (*Callithrix jacchus*): A study using cholera toxin subunit B. J Comp Neurol 415:393-403.

Cursiefen C, Holbach LM, Schlotzer U, Naumann GOH. 2001. Persisting retinal ganglion cell axons in blind atrophic human eyes. Graef Arch Clin Exp Opthalmol 239:158-164.

Czeisler CA, Shanahan TL, Klerman EB, Martens H, Brotman DJ, Emens JS, Klein T, Rizzo JF 3rd. 1995. Suppression of melatonin secretion in some blind patients by exposure to bright light. N Eng J Med 332:6-11.

Dacey DM, Liao HW, Peterson BB, Robinson FR, Smith VC, Pokorny J, Yau KW, Gamlin PD. 2005. Melanopsin-expressing ganglion cells in primate retina signal colour and irradiance and project to the LGN. Nature 433: 749-54.

Dacey DM, Peterson BB, Robinson FR, Gamlin PD. 2003. Fireworks in the primate retina: in vitro photodynamics reveals diverse LGN-projecting ganglion cell types. Neuron. 37:15-27

David-Gray Z.K., Cooper H.M., Janssen J.W., Nevo E., Foster R.G. 1999. Spectral tuning of a circadian photopigment in a subterranean 'blind' mammal (Spalax ehrenbergi). FEBS Lett 461:343-7.

Doi M, Uji Y, Yamamura H. 1995. Morphological classification of retinal ganglion cells in mice. J Comp Neurol. 1995 356: 368-86.

Dowling JE, Sidman RL, 1962. Inherited retinal dystrophy in the rat. J Cell Biol. 14:73-109

Doyle SE, Castrucci AM, McCall M, Provencio I, Menaker M. 2006. Nonvisual light responses in the Rpe65 knockout mouse: rod loss restores sensitivity to the melanopsin system. Proc Natl Acad Sci. 103:10432-10437.

Ebihara S, Tsuji K. 1980. Entrainment of the circadian activity rhythm to the light cycle: effective light intensity for a zeitgeber in the retinal degenerate C3H mouse and normal C57BL mouse. Physiol Behav 24:523-527.

Fahrenkrug J, Nielsen HS, Hannibal J. 2004. Expression of melanopsin during development of the rat retina. Neuroreport. 15:781-784.

Famiglietti EV, Kolb H. 1976. Structural basis for ON- and OFF-center responses in retinal ganglion cells. Science. 194:193-195.

Fisher LJ. 1979. Development of synaptic arrays in the inner plexiform layer of neonatal mouse retina. J Comp Neurol. 187:359-372.

Fite KV, Bengston CL, Baver SB, Blanchard J. 2003. Melanopsin immunoreactivity in the diurnal Mongolian gerbil. SfN Abstract.Field GD, Chichilnisky EJ. 2007. Information processing in the primate retina: circuitry and coding.Annu Rev Neurosci. 30:1-30.

Foster RG, Provencio I, Hudson D, Fiske S, De Grip W, Menaker M. 1991. Circadian photoreception in the retinally degenerate mouse (*rd/rd*). J Comp Physiol [A] 169:39-50.

Foster RG, Hankins MW. 2002. Non-rod, non-cone photoreception in the vertebrates. Prog Retin Eye Res. 2002 Nov;21(6):507-527.

Freedman MS, Lucas RJ, Soni B. 1999. Regulation of mammalian circadian behavior by non-rod, non-cone, ocular photoreceptors. Science 284:502-504.

Fu Y, Liao HW, Do MT, Yau KW. 2005. Non-image-forming ocular photoreception in vertebrates. Curr Opin Neurobiol 15:415-422.

Fukuda Y, Hsiao CF, Watanabe M. 1985. Morphological correlates of Y, X and W type ganglion cells in the cat's retina. Vision Res. 25: 319-32725:319-327.

Garcia-Fernandez JM, Jimenez AJ, Foster RG. 1995. The persistence of cone photoreceptors within the dorsal retina of aged retinally degenerate mice (*rd/rd*): implications for circadian organization. Neuroscience Lett 187: 33-36

Gooley JJ, Lu J, Chou TC, Scammell TE, Saper CB. 2001. Melanopsin in cells of origin of the retinohypothalamic tract. Nat Neurosci 12:1165.

Gooley JJ, Lu J, Fischer D, Saper CB. 2003. A broad role for melanopsin in nonvisual photoreception. J Neurosci 23: 7093-7106.

Göz D, Studholme K, Lappi DA, Rollag MD, Provencio I, Morin LP. 2008. Targeted destruction of photosensitive retinal ganglion cells with a saporin conjugate alters the effects of light on mouse circadian rhythms. PLoS One. 3:e3153.

Güler AD, Ecker JL, Lall GS, Haq S, Altimus CM, Liao HW, Barnard AR, Cahill H, Badea TC, Zhao H, Hankins MW, Berson DM, Lucas RJ, Yau KW, Hattar S. 2008. Melanopsin cells are the principal conduits for rod-cone input to non-image-forming vision. Nature. 453:102-105.

Hannibal J, Hindersson P, Nevo E, Fahrenkrug J. 2002a. The circadian photopigment melanopsin is expressed in the blind subterranean mole rat, *Spalax*. Neuroreport 13:1411-1414.

Hannibal J, Hindersson P, Knudsen SM, Georg B, Fahrenkrug J. 2002b. The photopigment melanopsin is exclusively present in pituitary adenylate cyclase-activating polypeptide-containing retinal ganglion cells of the retinohypothalamic tract.J Neurosci. 22:RC191.

Hannibal J, Hindersson P, Ostergaard J, Georg B, Heegaard S, Larsen PJ, Fahrenkrug J. 2004. Melanopsin is expressed in PACAP-containing retinal ganglion cells of the human retinohypothalamic tract. Invest Ophthalmol Vis Sci. 45:4202-4209.

Hannibal J, Fahrenkrug J. 2004. Melanopsin containing retinal ganglion cells are light responsive from birth. Neuroreport. 15: 2317-2320.

Hannibal J, Georg B, Hindersson P, Fahrenkrug J. 2005. Light and darkness regulate melanopsin in the retinal ganglion cells of the albino Wistar rat. J Mol Neurosci 227:147-155.

Hannibal J. 2006. Regulation of melanopsin expression. Chronobiol Int 23:159-166.

Hartline, HK. 1938. The responses of single optic nerve fibers of the vertebrate eye to illumination of the retina. Am. J. Physiol. 121: 400-415.

Hartwick ATE, Bramley JR, Yu J, Stevens KT, Allen CN, Baldridge WH, Sollars PJ, Pickard GE. 2007. Light-evoked calcium responses of isolated melanopsin-expressing retinal ganglion cells. J Neurosci. 27:13468-13468.

Hattar S, Liao HW, Takao M, Berson DM, Yau KW. 2002. Melanopsin-containing retinal ganglion cells: architecture, projections, and intrinsic photosensitivity. Science. 295:1065-1069.

Hattar S, Lucas RJ, Mrosovsky N, Thompson S, Douglas RH, Hankins MW, Lem J, Biel M, Hofmann F, Foster RG, Yau KW. 2003. Melanopsin and rod-cone photoreceptive systems account for all major accessory visual functions in mice. Nature 424:76-81.

Hattar S, Kumar M, Park A, Tong P, Tung J, Yau KW, Berson DM. 2006. Central projections of melanopsin-expressing retinal ganglion cells in the mouse. J Comp Neurol 497:326-49.

Hattar S, Ecker JL, Dumitrescu ON, Chen SK, Wong KY, Alam NM, Prusky GT, Berson DM. 2009. Functions and target innervations of distinct subtypes of melanopsin cells. ARVO Abstract. 5027/D703.

Hoshi H, Liu WL, Massey SC, Mills SL. 2009. ON inputs to the OFF layer: bipolar cells that break the stratification rules of the retina. J Neurosci. 29:8875-83.

Hubel DH, Wiesel TN. 1962. Receptive fields, binocular interaction and functional architecture in the cat's visual cortex. J Physiol. 160:106-154.

Ingham ES, Günhan E, Fuller PM, Fuller CA. 2009. Immunotoxin-induced ablation of melanopsin retinal ganglion cells in a non-murine mammalian model.J Comp Neurol. 516:125-140.

Isoldi MC, Rollag MD, Castrucci AML, Provencio I. 2005. Rhabdomeric phototransduction initiated by the vertebrate photopigment melanopsin. PNAS 102:1217- 1221.

Iwakabe H, Katsuura G, Ishibashi C, Nakanishi S. 1997. Impairment of pupillary responses and optokinetic nystagmus in the mGluR6-deficient mouse. Neuropharm 36:135-143.

Jenkins A, Munoz M, Tarttelin EE, Bellingham J, Foster RG, Hankins MW. 2003. VA opsin, melanopsin, and an inherent light response within retinal interneurons. Curr Bio 13:1269-1278.

Jimenez AJ, Garcia-Fernandez JM, Gonzalez B, Foster RG. 1996. The spatio-temporal pattern of photoreceptor degeneration in the aged rd/rd mouse retina. Cell Tissue Res 284:193-202.

Johnson RF, Morin LP, Moore RY. 1988. Retinohypothalamic projections in the hamster and rat demonstrated using cholera toxin. Brain Res 462:301-312.

Jusuf PR, Lee SC, Hannibal J, Grünert U. 2007. Characterization and synaptic connectivity of melanopsin-containing ganglion cells in the primate retina.Eur J Neurosci. 26:2906-2921.

Kaneko A, Shimazaki H. 1976 Synaptic transmission from photoreceptors to bipolar and horizontal cells in the carp retina. Cold Spring Harb Symp Quant Biol. 40:537-546.

Klerman EB, Shanahan TL, Brotman DJ, Rimmer DW, Emens JS, Rizzo JF, Czeisler CA. 2002. Photic resetting of the human circadian pacemaker in the absence of conscious vision. J Biol Rhythms 17:548-555.

Kolb H, Cuenca N, Dekorver L. 1991. Postembedding immunohistochemistry for GABA and glycine reveals the synaptic relationships of the dopaminergic amacrine cell of the cat retina. J Comp Neurol. 310: 267-284.

Kolb H, Linberg KA, Fisher SK. 1992. Neurons of the human retina: a Golgi study. J Comp Neurol. 318:147-187.

Koyanagi M, Kubokawa K, Tsukamoto H, Shichida Y, Terakita A. 2005. Cephalochordate melanopsin: evolutionary linkage between invertebrate visual cells and vertebrate photosensitive retinal ganglion cells. Curr Biol 15:1065-1069.

Kuffler SW. 1953. Discharge patterns and functional organization of the mammalian retina. J. Neurophysiol. 16: 37-68.

Kumbalasiri T, Provencio I. 2005. Melanopsin and other novel mammalian opsins. Exp Eye Res 81:368-375.

Lu J, Shiromani P, Saper CB. 1999. Retinal input to the sleep-active ventrolateral preoptic nucleus in the rat. Neuroscience. 93:209-214.

Lucas RJ, Foster RG. 1999. Neither functional rod photoreceptors nor rod or cone outer segments are required for the photic inhibition of pineal melatonin. Endocrinology 140:1520-1524.

Lucas RJ, Freedman MS, Munoz M, Garcia-Fernandez JM, Foster RG. 1999. Regulation of the mammalian pineal by non-rod, non-cone, ocular photoreceptors. Science 284:505-5077.

Lucas RJ, Douglas RH, Foster RG. 2001. Characterization of an ocular photopigment capable of driving pupillary constriction in mice. Nat Neurosci 4:621-626.

Lucas RJ, Hattar S, Takao M, Berson DM, Foster RG, Yau KW. 2003. Diminished pupillary light reflex at high irradiances in melanopsin-knockout mice. Science 299: 245-247.

Lupi D, Sekaran S, Jones SL, Hankins MW, Foster RG. 2006. Light-evoked FOS induction within the suprachiasmatic nuclei (SCN) of melanopsin knockout (Opn4-/-) mice: a developmental study. Chronobiol Int. 23:167-179.

Mariani AP. 1990. Amacrine cells of the rhesus monkey retina. J Comp Neurol. 15; 301:382-400.

Masland RH. 2001. The fundamental plan of the retina. Nat. Neurosci. 4: 877-886.

Maslim J, Stone J. 1988. Time course of stratification of the dendritic fields of ganglion cells in the retina of the cat. Brain Res Dev Brain Res. 44: 87-93.

Melyan Z, Tarttelin EE, Bellingham J, Lucas RJ, Hankins MW. 2005. Addition of human melanopsin renders mammalian cells photoresponsive. Nature 433:741-5.

Moore RY, Lenn NJ. 1972. A retinohypothalamic projection in the rat. J. Comp. Neurol.146: 1-14.

Morin LP, Blanchard JH, Provencio I. 2003. Retinal ganglion cell projections to the hamster suprachiasmatic nucleus, intergeniculate leaflet, and visual midbrain: bifuracation and melanopsin immunoreactivity. J Comp Neurol 465:401-416.

Mrosovsky N, Lucas RJ, Foster RG. 2001. Persistence of masking responses to light in mice lacking rods and cones. J Biol Rhythms 16:585-587.

Mrosovsky N. 2003. Contribution of classical photoreceptors to entrainment. J Comp Physiol. [A] 189:69-73.

Mrosovsky N, Hattar S. 2003. Impaired masking responses to light in melanopsin-knockout mice. Chron Bio Int 20:989-999.

Mumm JS, Godinho L, Morgan JL, Oakley DM, Schroeter EH, Wong RO. 2005. Laminar circuit formation in the vertebrate retina. Prog Brain Res. 147:155-169.

Nawy S, Jahr CE. 1990. Suppression by glutamate of cGMP-activated conductance in retinal bipolar cells. Nature. 346: 269-271.

Nelson R, Famiglietti EV, Kolb H. 1978. Intracellular staining reveals different levels of stratification for on- and off-center ganglion cells in cat retina. J Neurophysiol. 41:472-483.

Østergaard J, Hannibal J, Fahrenkrug J.2007. Synaptic contact between melanopsin-containing retinal ganglion cells and rod bipolar cells. Invest Ophthalmol Vis Sci. 48:3812-3820.

Pak MW, Giolli RA, Pinto LH, Mangini NJ, Gregory KM, Vanable JW. 1987. Retinopretectal and accessory optic projections of normal mice and the OKN-defective mutant mice beige, beige-J, and pearl. J. Comp. Neurol. 258: 435-446.

Panda S, Sato TK, Castrucci AM, Rollag MD, DeGrip WJ, Hogenesch JB, Provencio I, Kay SA. 2002. Melanopsin (Opn4) requirement for normal light-induced circadian phase shifting. Science 298:2213-2216.

Panda S, Provencio I, Tu DC, Pires SS, Rollag MD, Castrucci AM, Fletcher MT, Sato JK, Witshire T, Andahazy M, Kay SA., Van Gelder RN, Hogencsh JB. 2003. Melanopsin is required for non-image forming photic responses in blind mice. Science 298:2216-2220.

Panda S, Nayak SK, Campo B, Walker JR, Hogenesch JB, Jegla T. 2005. Illumination of the melanopsin signaling pathway. Science 307: 600-604.

Peichl L, Wässle H. 1981. Morphological identification of on- and off-centre brisk transient (Y) cells in the cat retina. Proc R Soc Lond B Biol Sci. 212:139-53.

Perry VH. 1979. The ganglion cell layer of the retina of the rat: a Golgi study. Proc R Soc Lond B Biol Sci. 204:363-75.

Perry VH, Oehler R, Cowey A. 1984.Retinal ganglion cells that project to the dorsal lateral geniculate nucleus in the macaque monkey. Neuroscience. 12:1101-1123.

Pickard GE. 1980. Morphological characteristics of retinal ganglion cells projecting to the suprachiasmatic nucleus: a horseradish peroxidase study. Brain Res. 183:458-65.

Pickard GE, Silverman AJ. 1981. Direct retinal projections to the hypothalamus, piriform cortex, and accessory optic nuclei in the golden hamster as demonstrated by a sensitive anterograde horseradish peroxidase technique. J Comp Neurol. 196:155-172.

Pickard GE. 1982. The afferent connections of the suprachiasmatic nucleus of the golden hamster with emphasis on the retinohypothalamic projection. J. Comp Neurol. 211: 65-83.

Pickard GE. 1985. Bifurcating axons of retinal ganglion cells terminate in the hypothalamic suprachiasmatic nucleus and the intergeniculate leaflet of the thalamus. Neurosci Lett 55:211-217.

Pickard GE, Ralph MR, Menaker, M. 1987. The intergeniculate leaflet partially mediates effects of light on circadian rhythms. J. Biol. Rhythms, 2: 35-56.

Pickard GE, Smeraski CA, Tomlinson CC, Banfield BW, Kaufman J, Wilcox CL, Enquist LW, Sollars PJ. 2002. Intravitreal injection of the attenuated pseudorabies virus PRV Bartha results in infection of the hamster suprachiasmatic nucleus only by retrograde transsynaptic transport via autonomic circuits. J. Neurosci. 22: 2701-2710.

Pickard GE, Baver SB, Ogilvie MD, Sollars PJ. 2009. Light-induced fos expression in intrinsically photosensitive retinal ganglion cells in melanopsin knockout (opn4) mice. PLoS One. 4:e4984.

Provencio I, Foster RG. 1995. Circadian rhythms in mice can be regulated by photoreceptors with cone-like characteristics. Brain Res 694: 183-190.

Provencio I, Cooper HM, Foster RG. 1998a. Retinal projections in mice with inherited retinal degeneration: implications for circadian photoentrainment. J Comp Neurol 395: 417-439.

Provencio I, Jiang G, De Grip WJ, Hayes WR, Rollag MD. 1998b. Melanopsin: an opsin in melanophores, brain, and eye. Neurobiol 95:340-345.

Provencio I, Rodriguez IR, Jiang G, Hayes WP, Moreira EF, Rollag MD. 2000. A novel human opsin in the inner retina. J Neurosci 20:600-5.

Provencio I, Rollag MD, Castrucci AM. 2002a. Photoreceptive net in the mammalian retina. Nature 415:493.

Provencio I, Berson DM, Richardson RC, Rollag MD, Castrucci AM. 2002b. Melananopsin immunoreactivity in retinal ganglion cells. ARVO abstract.

Pu M. 1999. Dendritic morphology of cat retinal ganglion cells projecting to suprachiasmatic nucleus. J Comp Neurol 414: 267-274.

Ratto GM, Robinson DW, Yan B, McNaughton PA. 1991. Development of the light response in neonatal mammalian rods. Nature. 351:654-7.

Rea MS, Bullough JD, Figueiro MG. 2001. Human melatonin suppression by light: a case for scotopic efficiency.Neurosci Lett 299:45-8.

Reuss S, Fuchs E. 2000. Anterograde tracing of retinal afferents to the tree shrew hypothalamus and raphe. Brain Res 874:66-74.

Rodieck RW, Watanabe M. 1993. Survey of the morphology of macaque retinal ganglion cells that project to the pretectum, superior colliculus, and parvicellular laminae of the lateral geniculate nucleus. J Comp Neurol. 338:289-303.

Rollag MD, Provencio I, Sugden D, Green CA. 2000. Cultured amphibian melanophores: a model system to study melanopsin in photobiology. Methods Enzymol 316:291-309

Ruggiero L, Allen CN, Lane Brown R, Robinson DW. 2009. The development of melanopsin-containing retinal ganglion cells in mice with early retinal degeneration. Eur J Neurosci. 29: 359-367.

Ruby NF, Brennan TJ, Xie X, Cao V, Franken P, Heller HC, O'Hara BF. 2002. Role of melanopsin in circadian responses to light. Science 298:2211-2213.

Saito T, Kaneko A. 1983. Ionic mechanisms underlying the responses of off-center bipolar cells in the carp retina. I. Studies on responses evoked by light. J Gen Physiol. 81:589-601.

Sakamoto K, Liu C, Tosini G. 2004. Classical photoreceptors regulate *melanopsin* mRNA levels in the rat retina. J Neurosci 24:9693-9697.

Sakamoto K, Liu C, Kasamatsu M, Pozdeyev NV, Iuvone PM, Tosini G. 2005. Dopamine regulates melanopsin mRNA expression in intrinsically photosensitive retinal ganglion cells. Eur J Neurosci 22:3129-3136.

Scalia F. 1972. The termination of retinal axons in the pretectal region of mammals. J. Comp. Neurol. 145: 223-257.

Scalia F, Arango, V. 1979.Topographic organization of the projections of the retina to the pretectal region in the rat. J. Comp. Neurol. 186: 272-291.

Schmidt TM, Taniguchi K, Kofuji P. 2008. Intrinsic and extrinsic light responses in melanopsin-expressing ganglion cells during mouse development. J. Neurophysiol. 100:371-384.

Schmidt TM, Kofuji PJ. 2009. Functional and morphological differences among intrinsically photosensitive retinal ganglion cells. J. Neurosci. 29:476-482.

Sekaran S, Foster RG, Lucas RJ, Hankins MW. 2003. Calcium imaging reveals a network of intrinsically light-sensitive inner-retinal neurons. Curr Biol 13:1290-1298.

Sekeran S, Lupi D, Jones SL, Sheely CJ, Hattar S, Yau KW, Lucas RJ, Foster RG, Hankins MW. 2005. Melanopsin-dependent photoreception provides earliest light detection in the mammalian retina. Curr Biol. 15:1099-1107.

Semo M, Peirson S, Lupi D, Lucas RJ, Jeffery G, Foster RG. 2003a. Melanopsin retinal ganglion cells and the maintenance of circadian and pupillary responses to light in aged rodless/coneless (*rd/rd cl*) mice. Eur J Neurosci 17:1793-1801.

Semo M, Lupi D, Peirson SN, Butler JN, Foster RG. 2003b Light-induced c-fos in melanopsin retinal ganglion cells of young and aged rodless/coneless (rd/rd cl) mice. Eur J Neurosci. 18: 3007-3017.

Semo M, Muñoz Llamosas M, Foster RG, Jeffery G. 2005. Melanopsin (Opn4) positive cells in the cat retina are randomly distributed across the ganglion cell layer. Vis Neurosci. 22: 111-116.

Shiells RA, Falk G.1990. Glutamate receptors of rod bipolar cells are linked to a cyclic GMP cascade via a G-protein. Proc Biol Sci. 242: 91-94.

Smeraski CA, Sollars PJ, Ogilvie MD, Enquist LW, Pickard GE. 2004. Suprachiasmatic nucleus input to autonomic circuits identified by retrograde transsynaptic transport of pseudorabies virus from the eye. J Comp Neurol. 471: 298-313.

Smith BN, Banfield BW, Smeraski CA, Wilcox CL, Dudek FE, Enquist LW, Pickard GE. 2000. Pseudorabies virus expressing enhanced green fluorescent protein: A tool for in vitro electrophysiological analysis of transsynaptically labeled neurons in identified central nervous system circuits. Proc. Natl. Acad. Sci.,97: 9264-9269.

Snellman J, Kaur T, Shen Y, Nawy S. 2008.Regulation of ON bipolar cell activity. Prog Retin Eye Res. 27: 450-63.

Sollars PJ, Ogilvie MD, Rea MA, Pickard GE. 2002. 5-HT1B receptor knockout mice exhibit an enhanced response to constant light.. J Biol Rhythms. 17:428-437

Sollars PJ, Smeraski CA, Kaufman JD, Ogilvie MD, Provencio I, Pickard GE. 2003. Melanopsin and non-melanopsin expressing retinal ganglion cells innervate the hypothalamic suprachiasmatic nucleus.Vis Neurosci 20:601-610.

Stone J, Clarke R. 1980. Correlation between soma size and dendritic morphology in cat retinal ganglion cells: evidence of further variation in the gamma-cell class. J Comp Neurol.192:211-217.

Sun W, Li N, He S. 2002a. Large-scale morophological survey of rat retinal ganglion cells. Vis Neurosci. 19:483-493.

Sun W, Li N, He S. 2002b. Large-scale morphological survey of mouse retinal ganglion cells. J Comp Neurol. 451:115-126.

Takao M, Morigiwa K, Sasaki H, Miyoshi T, Shima T, Nakanishi S, Nagai K, Fukuda Y. 2000. Impaired behavioral suppression by light in metabotropic glutamate receptor subtype 6-deficient mice. Neurosci 97:779-787.

Tian N. 2008. Synaptic Activity, visual experience and the maturation of retinal synaptic circuitry. J Physiol. 586:4347-4355

Tian N, Copenhagen DR. 2003. Visual stimulation is required for refinement of ON and OFF pathways in postnatal retina. Neuron 39: 85-96.

Thapan K, Arendt J, Skene DJ. 2001. An action spectrum for melatonin suppression: evidence for a novel non-rod, non-cone photoreceptor system in humans. J Physiol 535: 261-267.

Trejo LJ, Cicerone CM. 1984. Cells in the pretectal olivary nucleus are in the pathway for the direct light reflex of the pupil in the rat. Brain. Res. 300: 49-62.

Trifonov IU. 1968.Study of synaptic transmission between photoreceptor and horizontal cell by electric stimulations of the retina. Biofizika. 13:809-817

Tu DC, Zhang D, Demas J, Slutsky EB, Provencio I, Holy TE, Van Gelder RN. 2005. Physiologic diversity and development of intrinsically photosensitive retinal ganglion cells. Neuron. 48:987-999.

Van Gelder RN. 2003. Making (a) sense of non-visual ocular photoreception. Trends Neurosci. 26:458-461.

Viney TJ, Balint K, Hillier D, Siegert S, Boldogkoi Z, Enquist LW, Meister M, Cepko CL, Roska B. 2007. Local retinal circuits of melanopsin-containing ganglion cells identified by transsynaptic viral tracing. Curr Biol. 17:981-988.

Voigt T, Wässle H.1987. Dopaminergic innervation of AII amacrine cells in mammalian retina. J Neurosci. 7:4115-4128.

von Schantz M, Argamaso-Hernan SM, Szel A, Foster RG. 1997. Photopigments and photoentrainment in the Syrian golden hamster. Brain Res 770:131-138.

von Schantz M, Provencio I, Foster RG. 2000. Recent developments in circadian photoreception: more than meets the eye. Invest Ophthalmol Vis Sci. 41(7):1605-1607.

Vugler AA, Redgrave P, Semo M, Lawrence J, Greenwood J, Coffey PJ.2007. Dopamine neurones form a discrete plexus with melanopsin cells in normal and degenerating retina. Exp Neurol. 205:26-35.

Vugler AA, Semo M, Joseph A, Jeffery G. 2008. Survival and remodeling of melanopsin cells during retinal dystrophy. Vis Neurosci. 25:125-138.

Wong KY, Dunn FA, Graham DM, Berson DM. 2007. Synaptic influences on rat ganglion-cell photoreceptors. 582:279-296.

Wong RO, Ghosh A. 2002. Activity-dependent regulation of dendritic growth and patterning. Nat Rev Neurosci. 3:803-812.

Wan J, Zheng H, Hu BY, Xiao HL, She ZJ, Chen ZL, Zhou GM.2006. Acute photoreceptor degeneration down-regulates melanopsin expression in adult rat retina. Neurosci Lett. 400:48-52.

Warren EJ, Allen CN, Brown RL, Robinson DW. 2003. Intrinsic light responses of retinal ganglion cells projecting to the circadian system. Eur J Neurosci. 17: 1727-1735.

Wässle H, Peichl L, Boycott BB. 1981a. Morphology and topography of on- and off-alpha cells in the cat retina. Proc R Soc Lond B Biol Sci. 212:157-175.

Wässle H, Peichl L, Boycott BB. 1981b. Dendritic territories of cat retinal ganglion cells. Nature. 292:344-345.

Wässle H. 2004. Parallel processing in the mammalian retina.Nat Rev Neurosci. 5:747-757.

Werblin FS, Dowling JE. 1969. Organization of the retina of the mudpuppy. *Nectorus maculosus*. II. Intracellular recording. J Neurophysiol. 29: 1115-1156.

Witkovsky P. 2004. Dopamine and retinal function. Doc Ophthalmol 108:17-40.

Wong KY, Dunn FA, Graham DM, Berson DM. 2007. Synaptic influences on rat ganglion-cell photoreceptors. J Physiol. 582:279-296.

Wulle I, Schnitzer J. 1989. Distribution and morphology of tyrosine hydroxylase-immunoreactive neurons in the developing mouse retina. Dev Brain Res. 48: 59-72.

Young MJ, Lund RD. 1998. The retinal ganglion cells that drive the pupilloconstrictor response in rats. Brain Res 787:191-202.

Zhang DQ, Wong KY, Sollars PJ, Berson DM, Pickard GE, McMahon DG. 2008. Intraretinal signaling by ganglion cell photoreceptors to dopaminergic amacrine neurons. Proc Natl Acad Sci USA. 105: 14181-14186.